Bayesianize Fuzziness in the Statistical Analysis of Fuzzy Data

Antonio Calcagnì*, Przemysław Grzegorzewski, Maciej Romaniuk

Supplementary Materials

Contents

*Corresponding author: antonio.calcagni@unipd.it

1 Extended results for Section 5 (Simulation Study)

This section contains extended graphical results for the approximation problem of the posterior density function $\pi(y|\boldsymbol{\theta_y}, \mathbf{D})$ described in Section 5 of the main article. The graphical results are reported in Figures S.1-S.20.

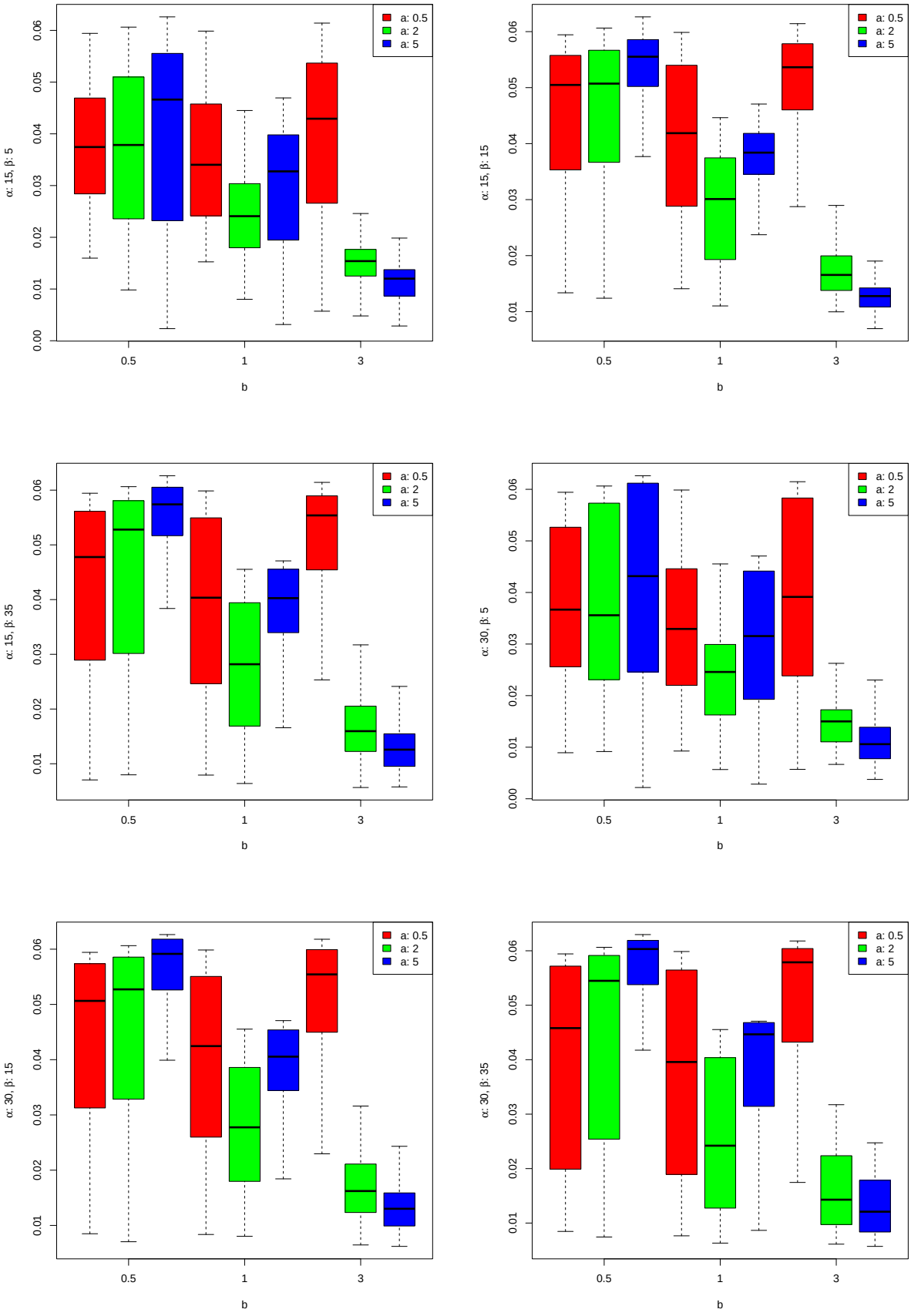

Figure S.1: Boxplots for the estimated total variation (TV) distance in the DA analysis for $\mathcal{B}(a, b)$.

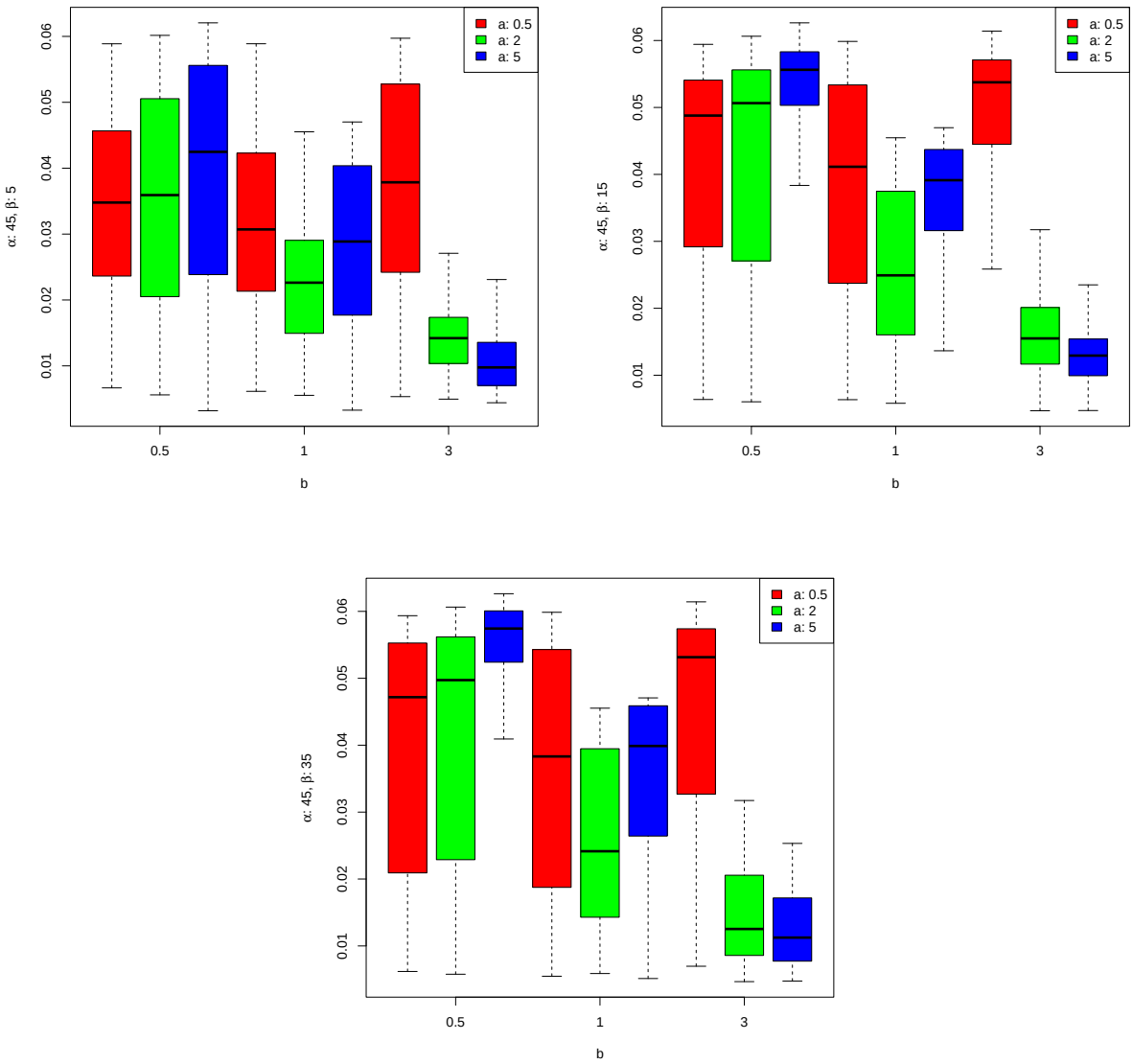

Figure S.2: Boxplots for the estimated total variation (TV) distance in the DA analysis for $\mathcal{B}(a, b)$ (continuation).

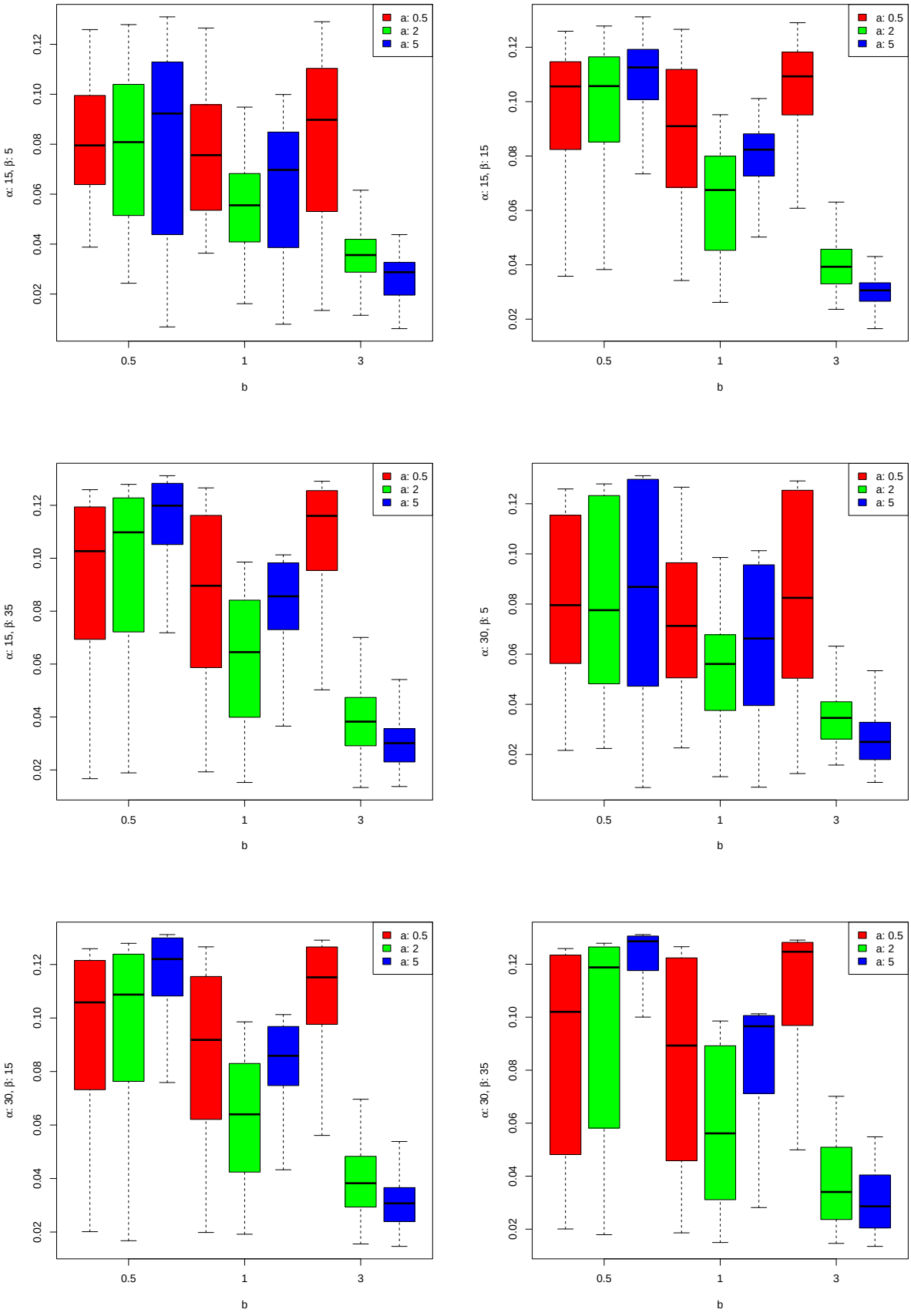

Figure S.3: Boxplots for the estimated Hellinger distance (HD) in the DA analysis for $\mathcal{B}(a, b)$.

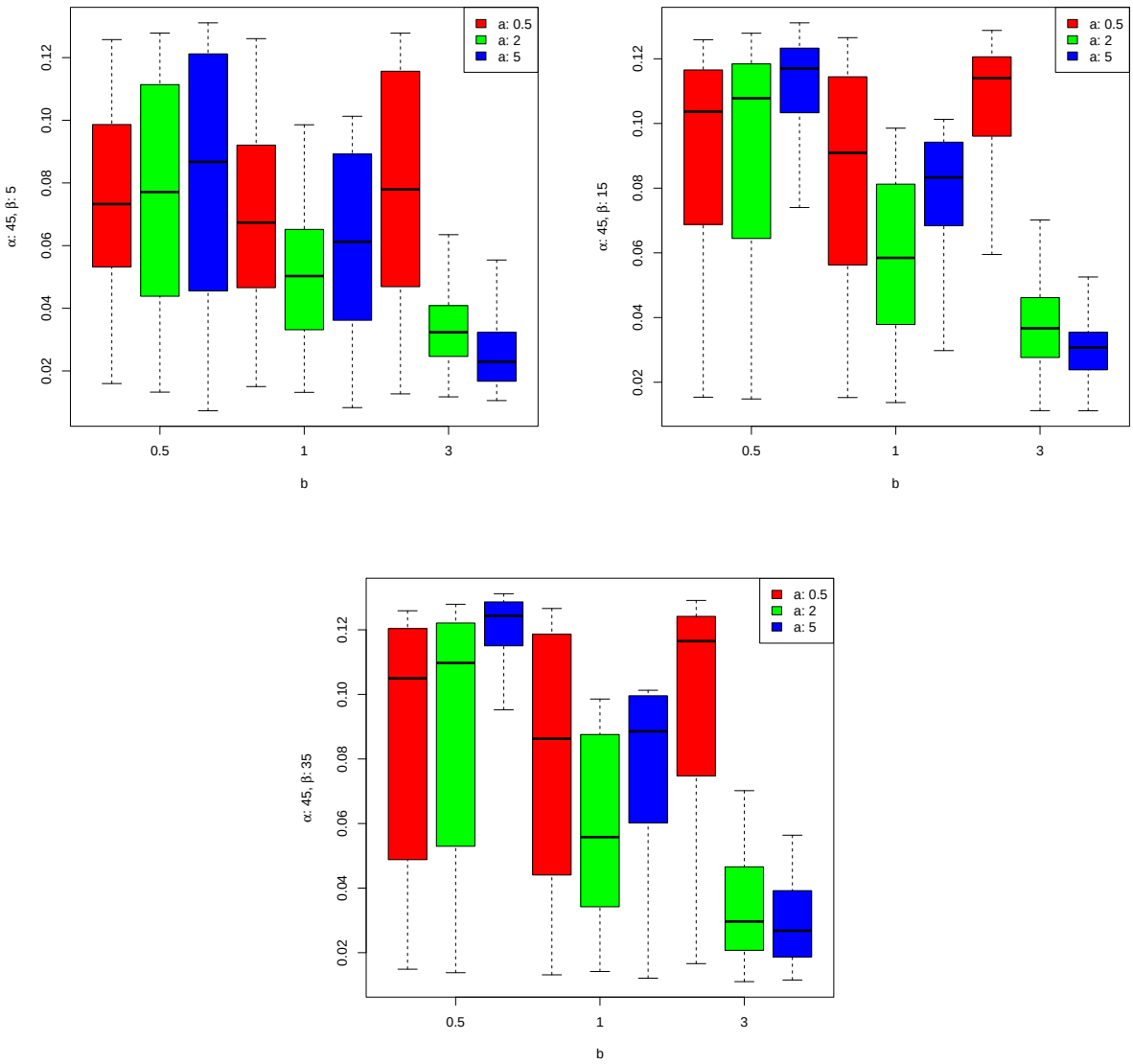

Figure S.4: Boxplots for the estimated Hellinger distance (HD) in the DA analysis for $\mathcal{B}(a, b)$ (continuation).

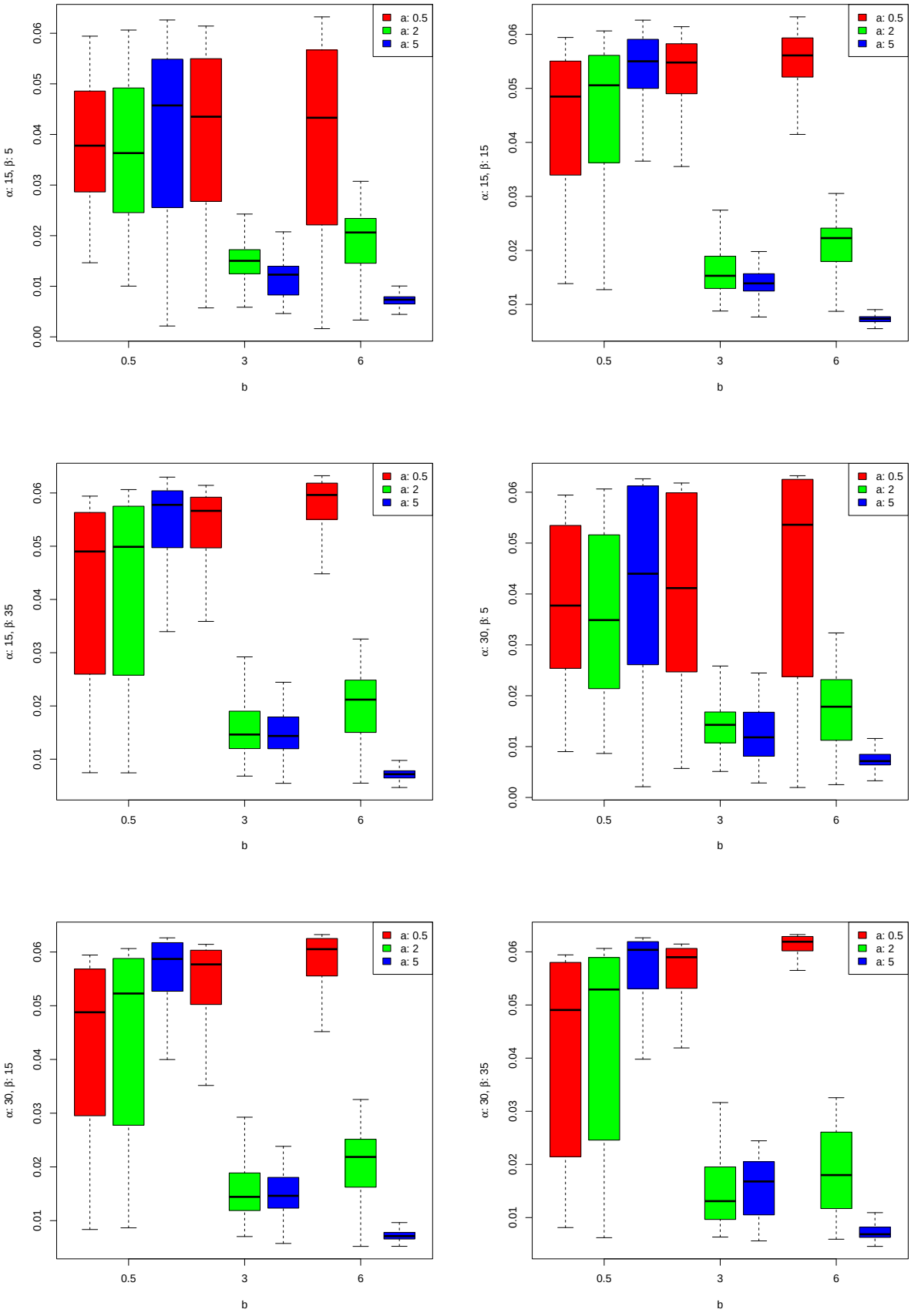

Figure S.5: Boxplots for the estimated total variation (TV) distance in the DA analysis for $\mathcal{K}(a, b)$.

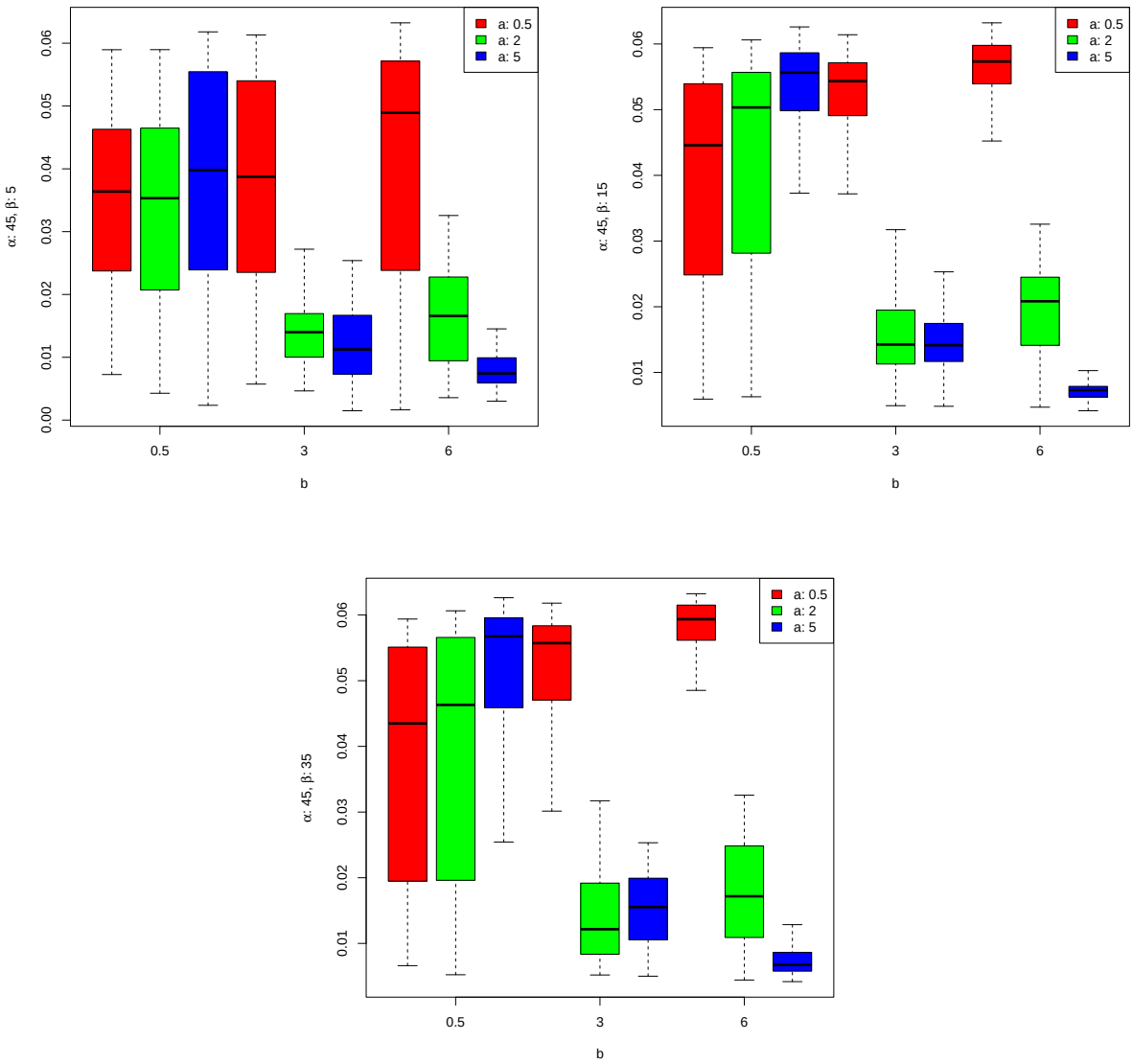

Figure S.6: Boxplots for the estimated total variation (TV) distance in the DA analysis for $\mathcal{K}(a, b)$ (continuation).

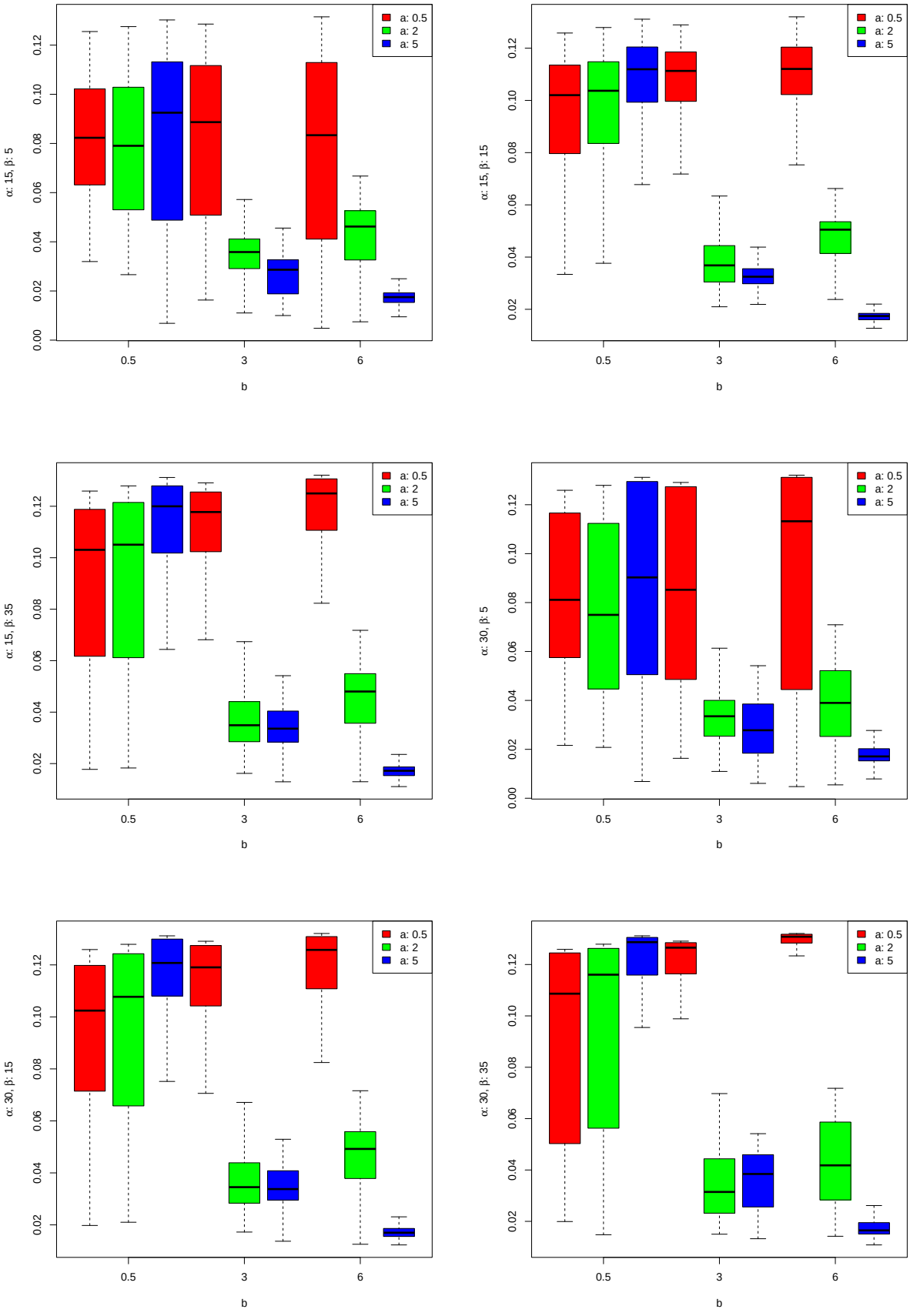

Figure S.7: Boxplots for the estimated Hellinger distance (HD) in the DA analysis for $\mathcal{K}(a, b)$.

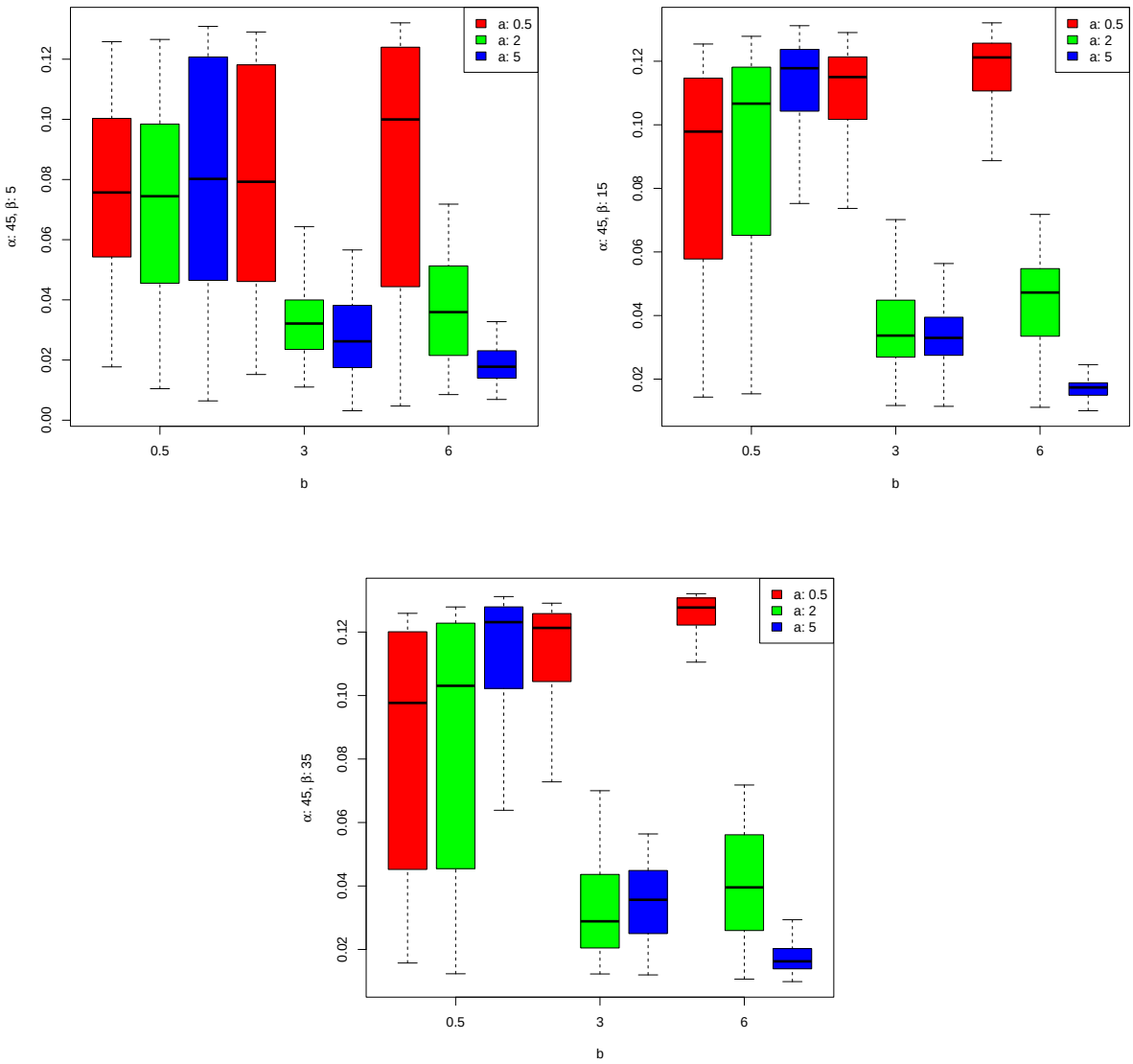

Figure S.8: Boxplots for the estimated Hellinger distance (HD) in the DA analysis for $\mathcal{K}(a, b)$ (continuation).

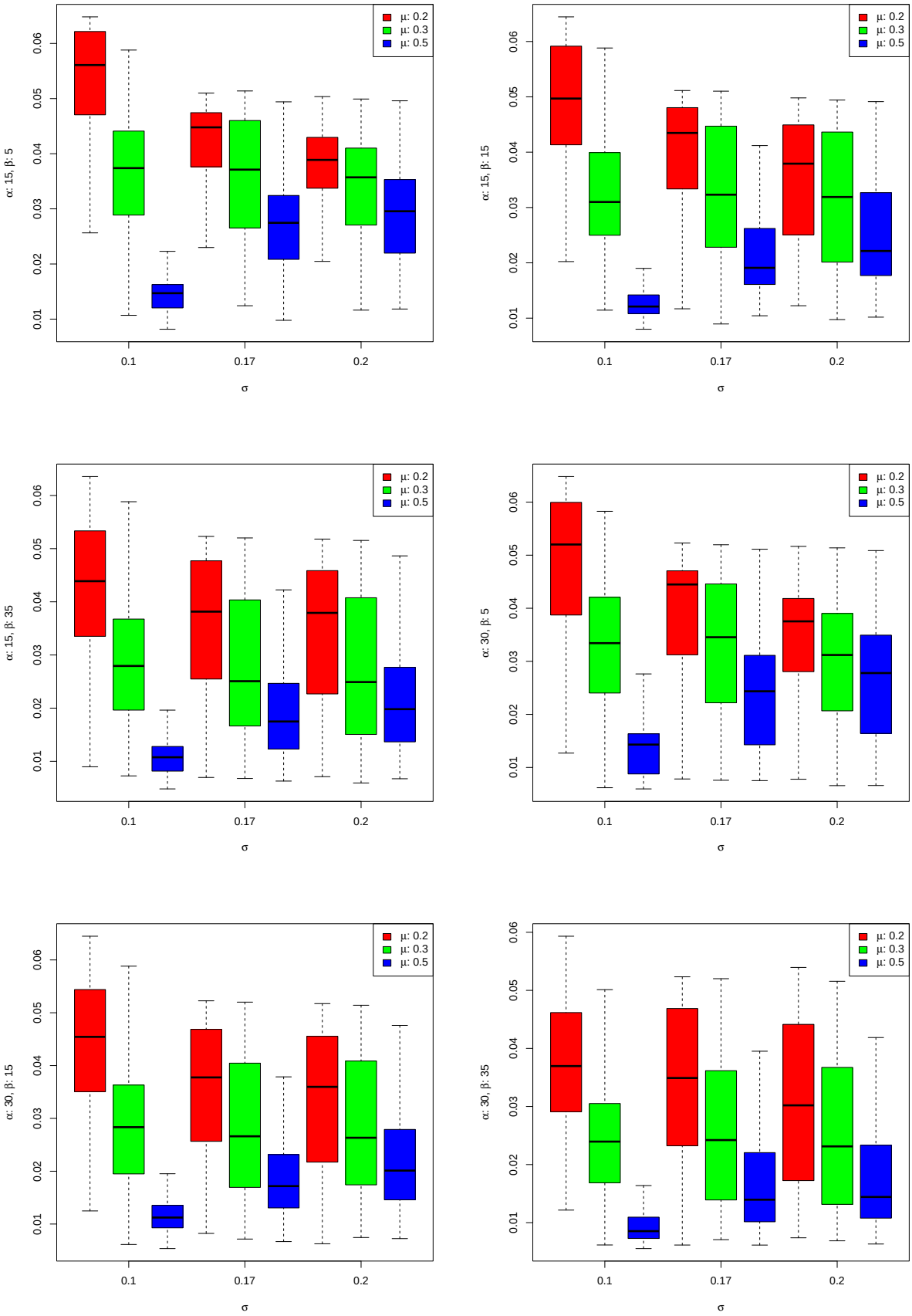

Figure S.9: Boxplots for the estimated total variation (TV) distance in the DA analysis for $\mathcal{TN}(a, b, \mu, \sigma)$.

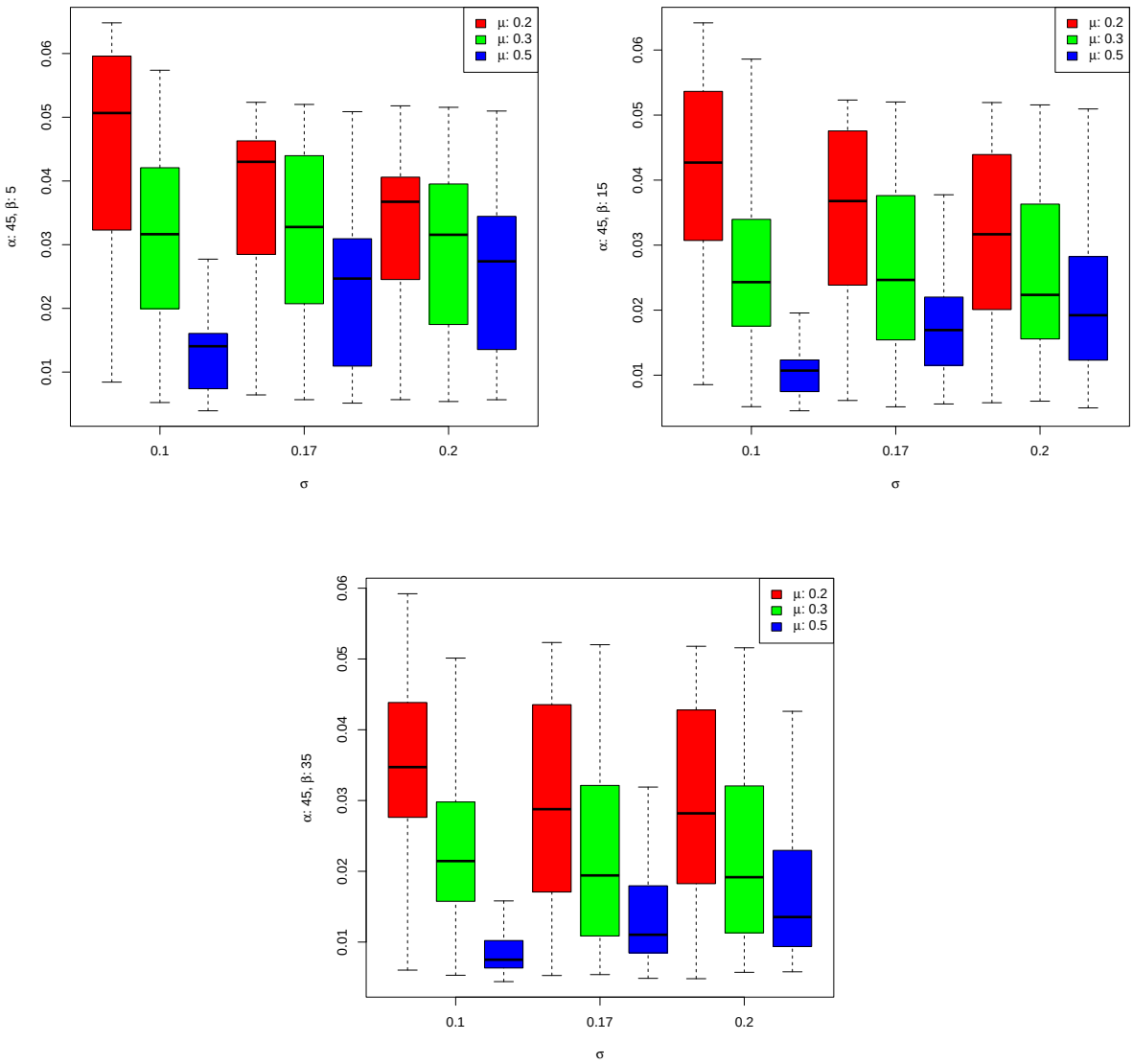

Figure S.10: Boxplots for the estimated total variation (TV) distance in the DA analysis for $\mathcal{TN}(a, b, \mu, \sigma)$ (continuation).

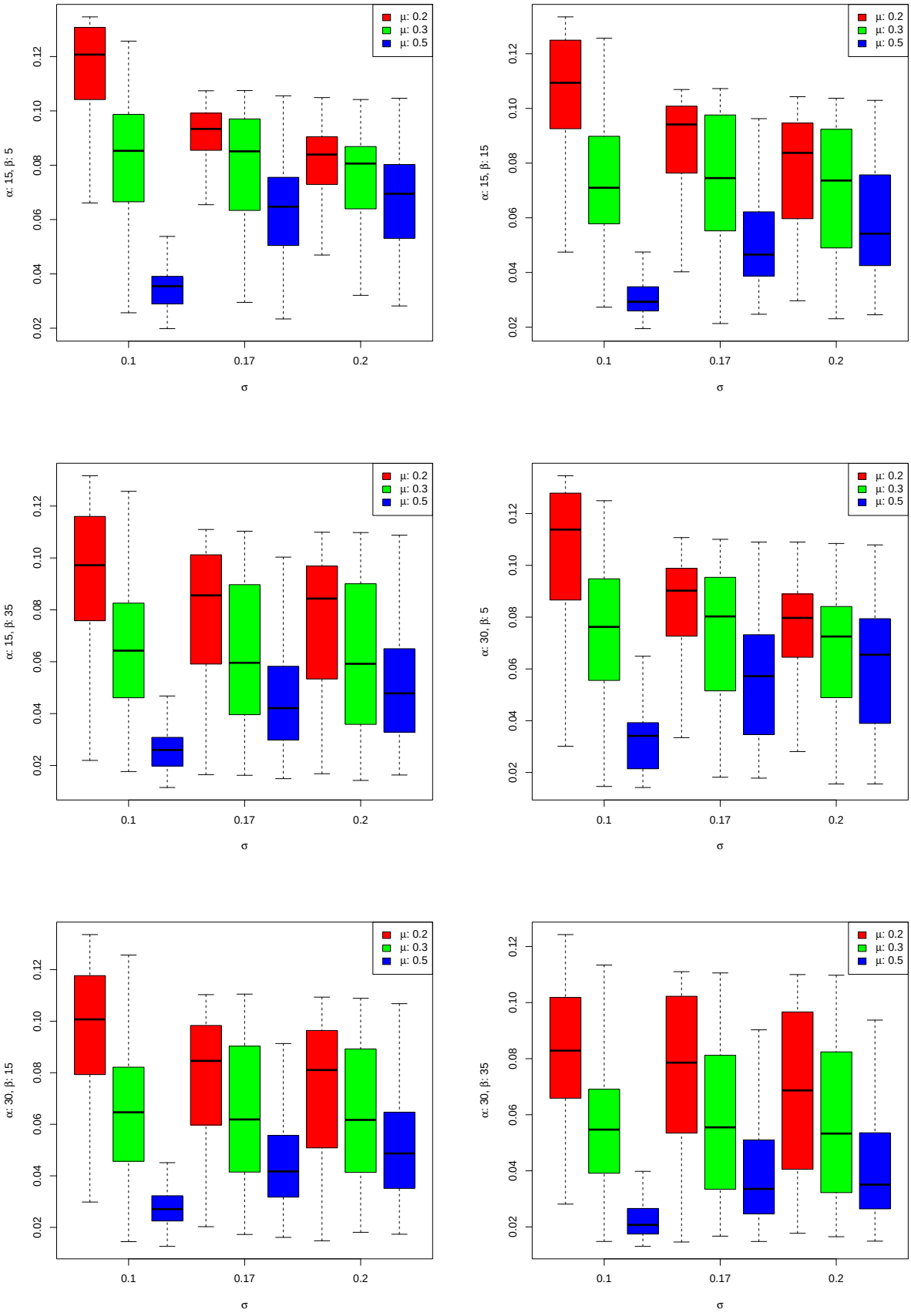

Figure S.11: Boxplots for the estimated Hellinger distance (HD) in the DA analysis for $\mathcal{TN}(a, b, \mu, \sigma)$.

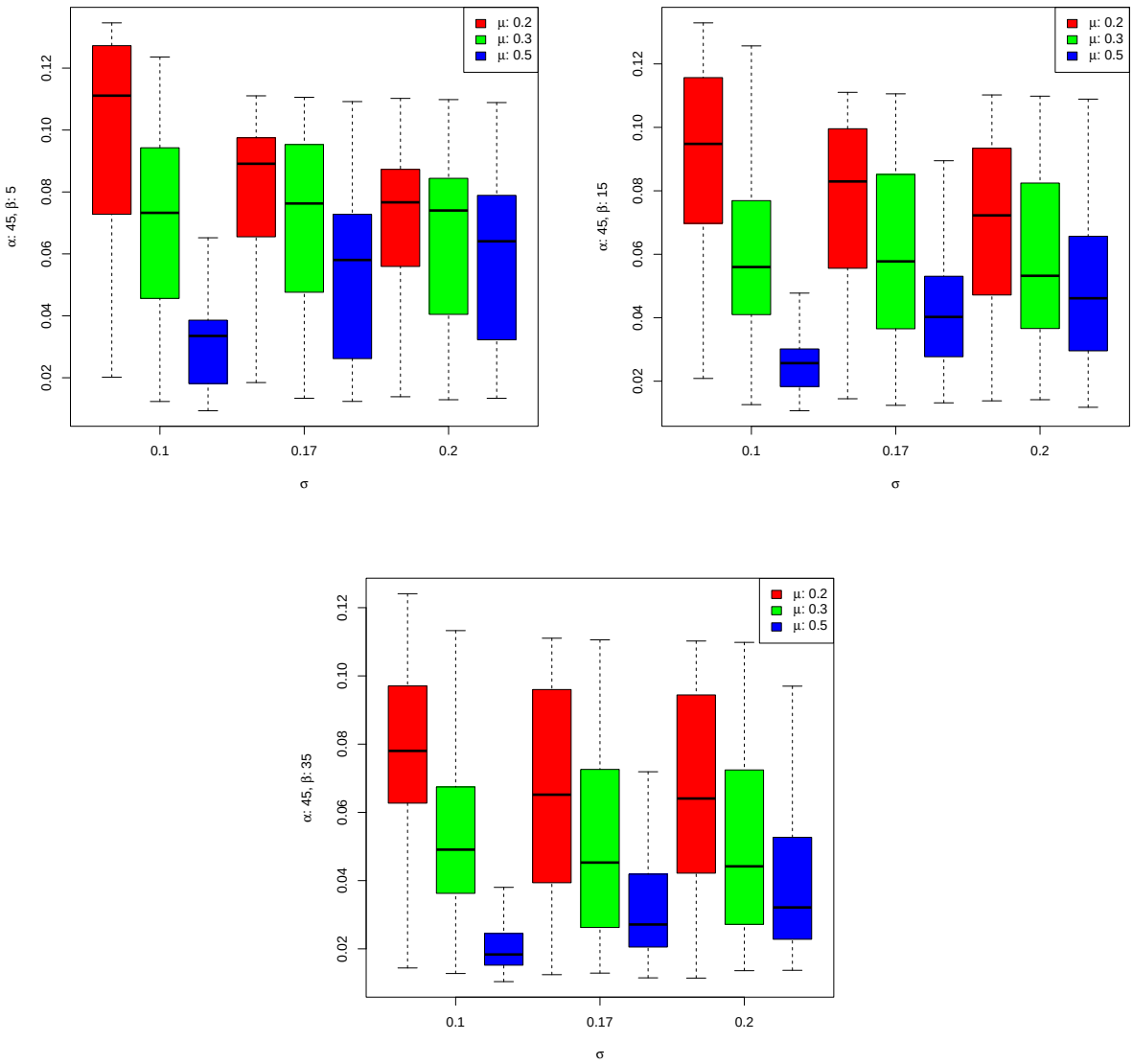

Figure S.12: Boxplots for the estimated Hellinger distance (HD) in the DA analysis for $\mathcal{TN}(a, b, \mu, \sigma)$ (continuation).

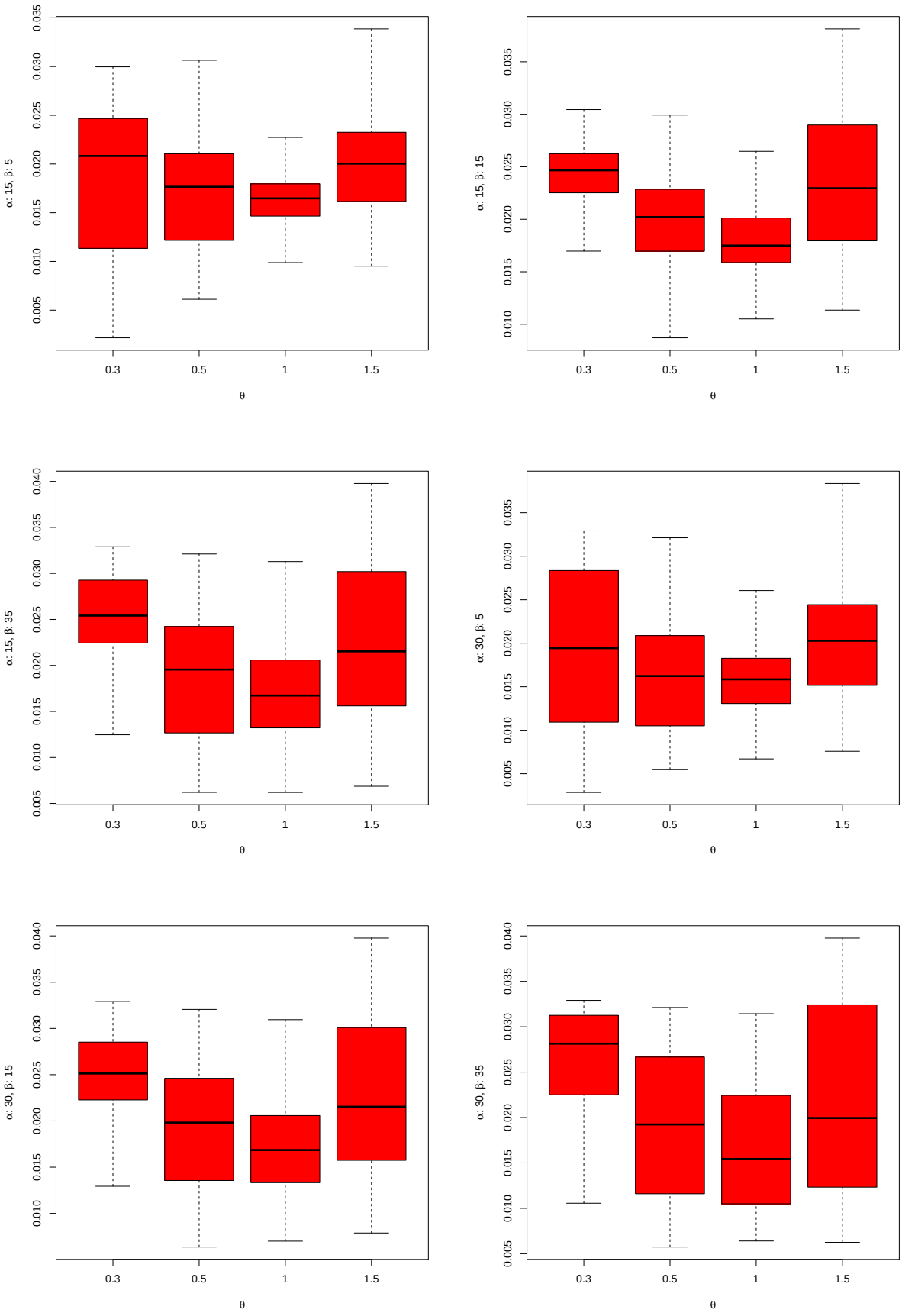

Figure S.13: Boxplots for the estimated total variation (TV) distance in the DA analysis for $\mathcal{LBL}(\theta)$.

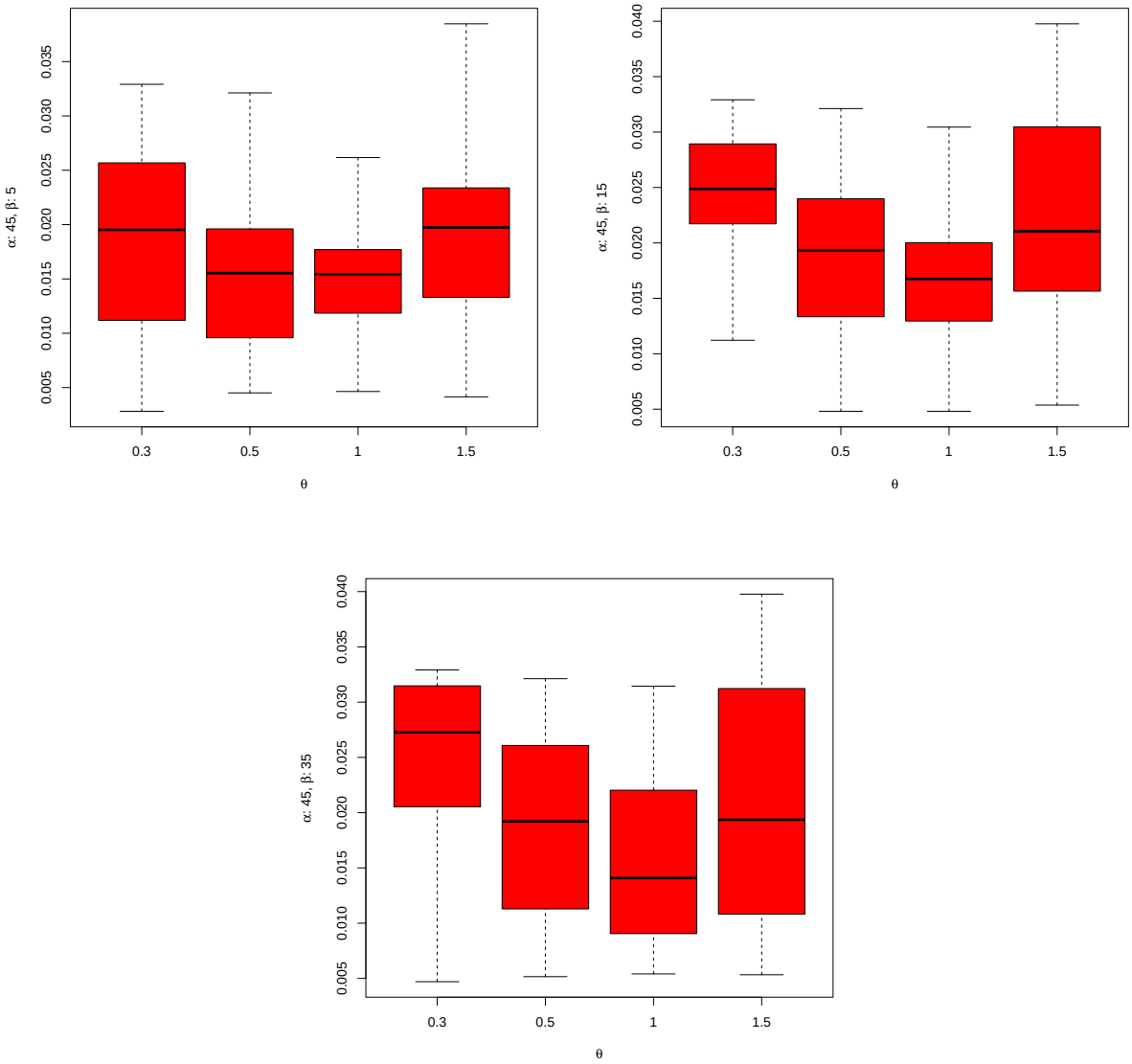

Figure S.14: Boxplots for the estimated total variation (TV) distance in the DA analysis for $\mathcal{LBL}(\theta)$ (continuation).

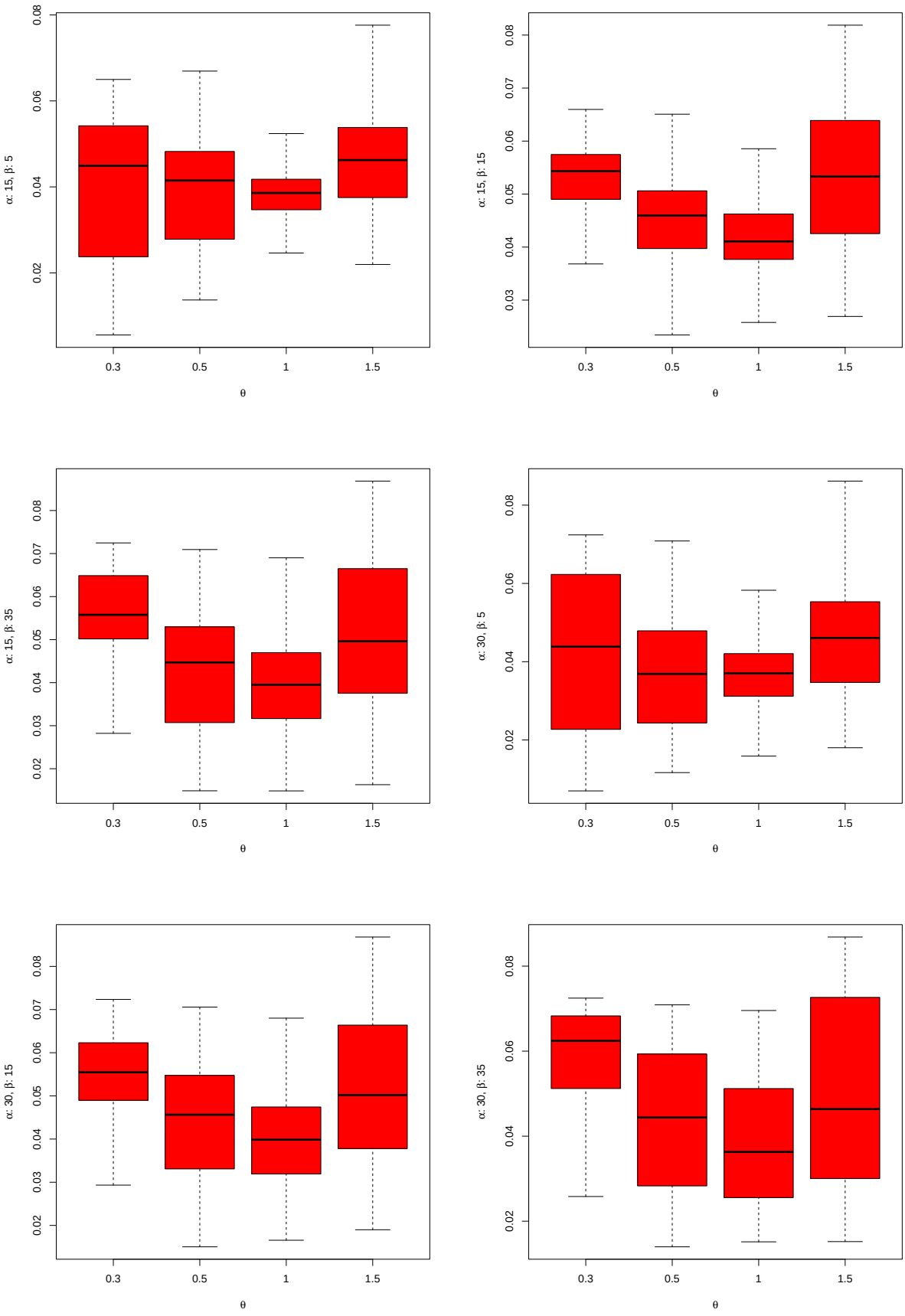

Figure S.15: Boxplots for the estimated Hellinger distance (HD) in the DA analysis for $\mathcal{LBL}(\theta)$.

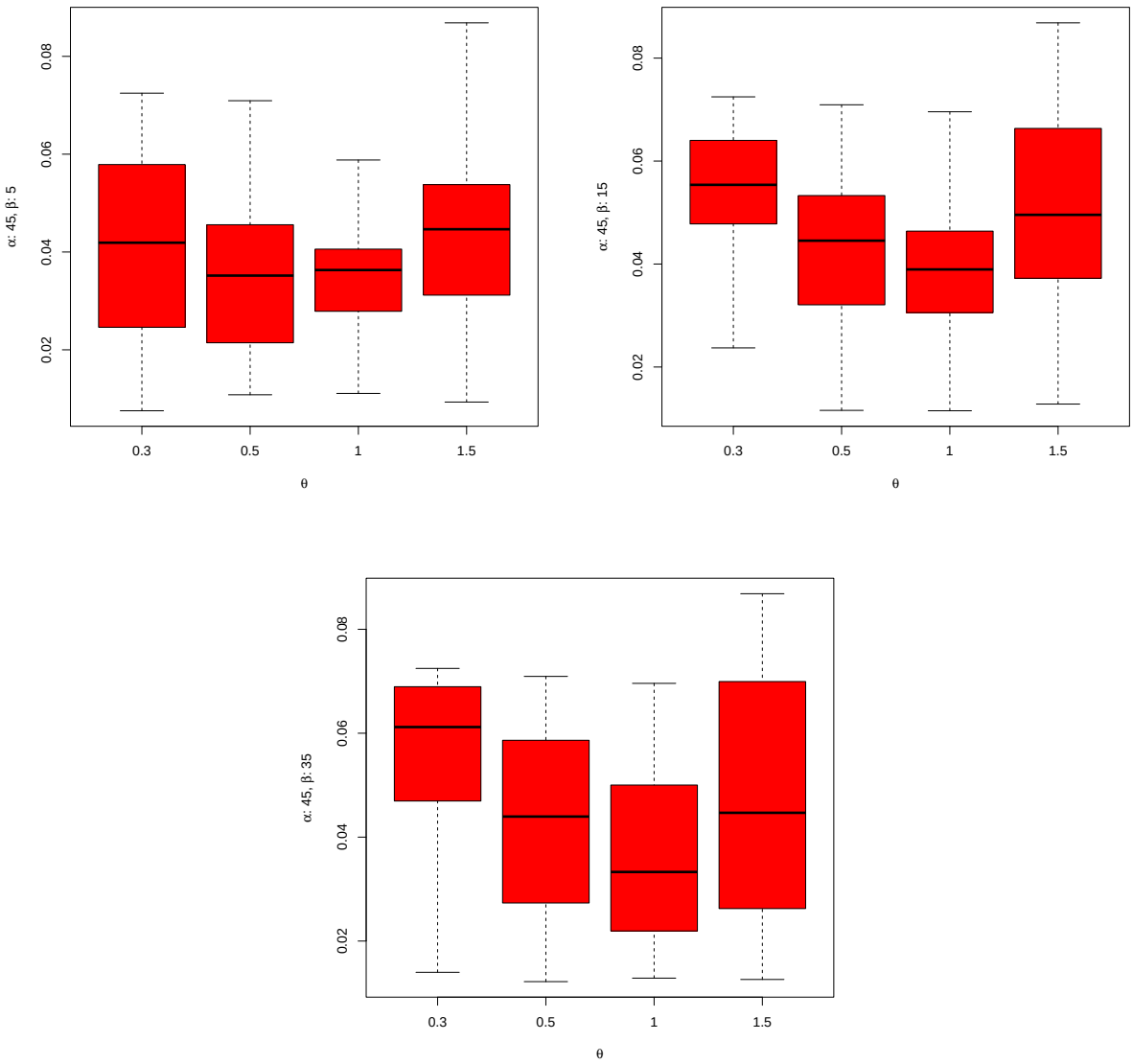

Figure S.16: Boxplots for the estimated Hellinger distance (HD) in the DA analysis for $\mathcal{LBL}(\theta)$ (continuation).

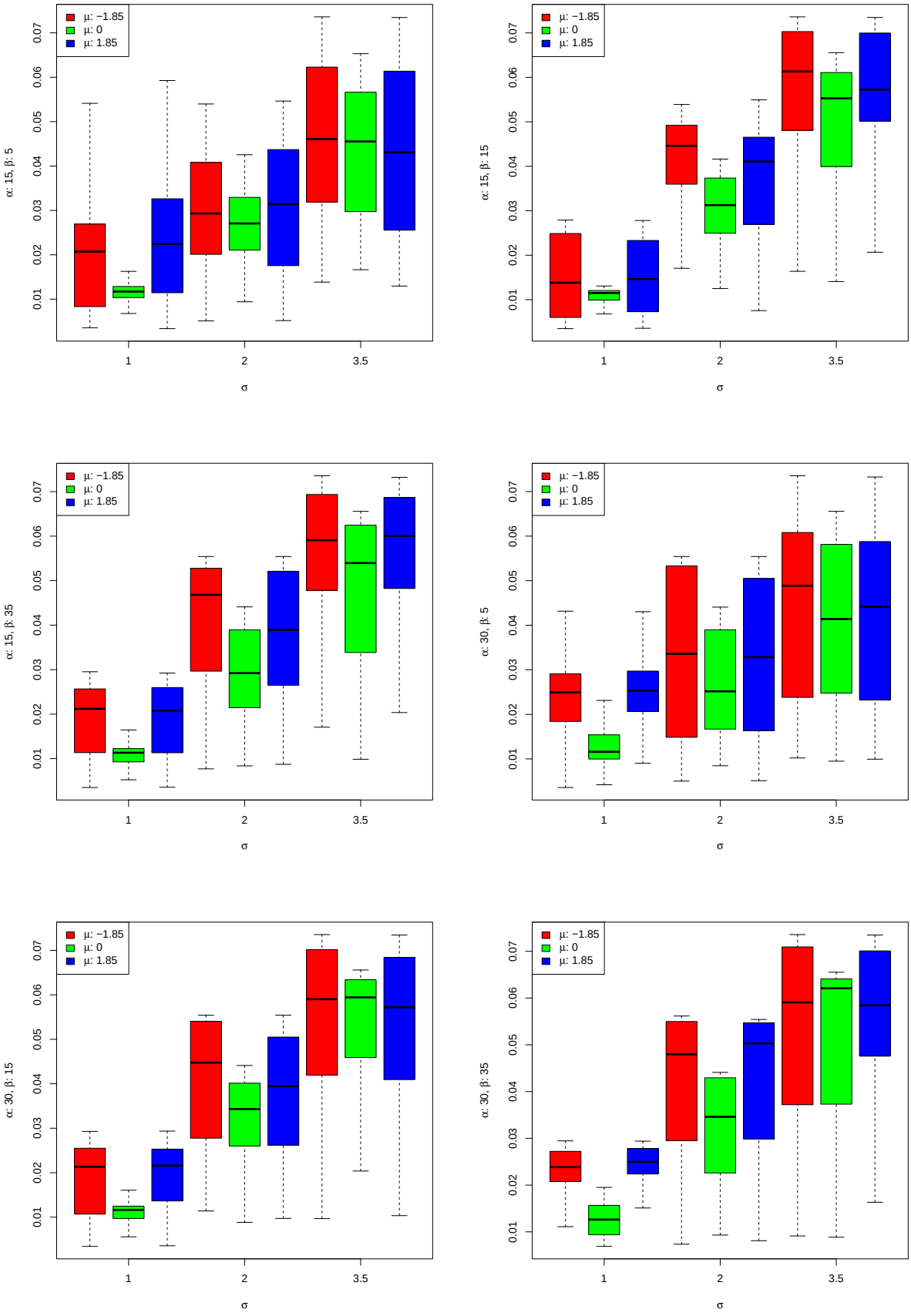

Figure S.17: Boxplots for the estimated total variation (TV) distance in the DA analysis for $\mathcal{LGN}(\mu, \sigma)$.

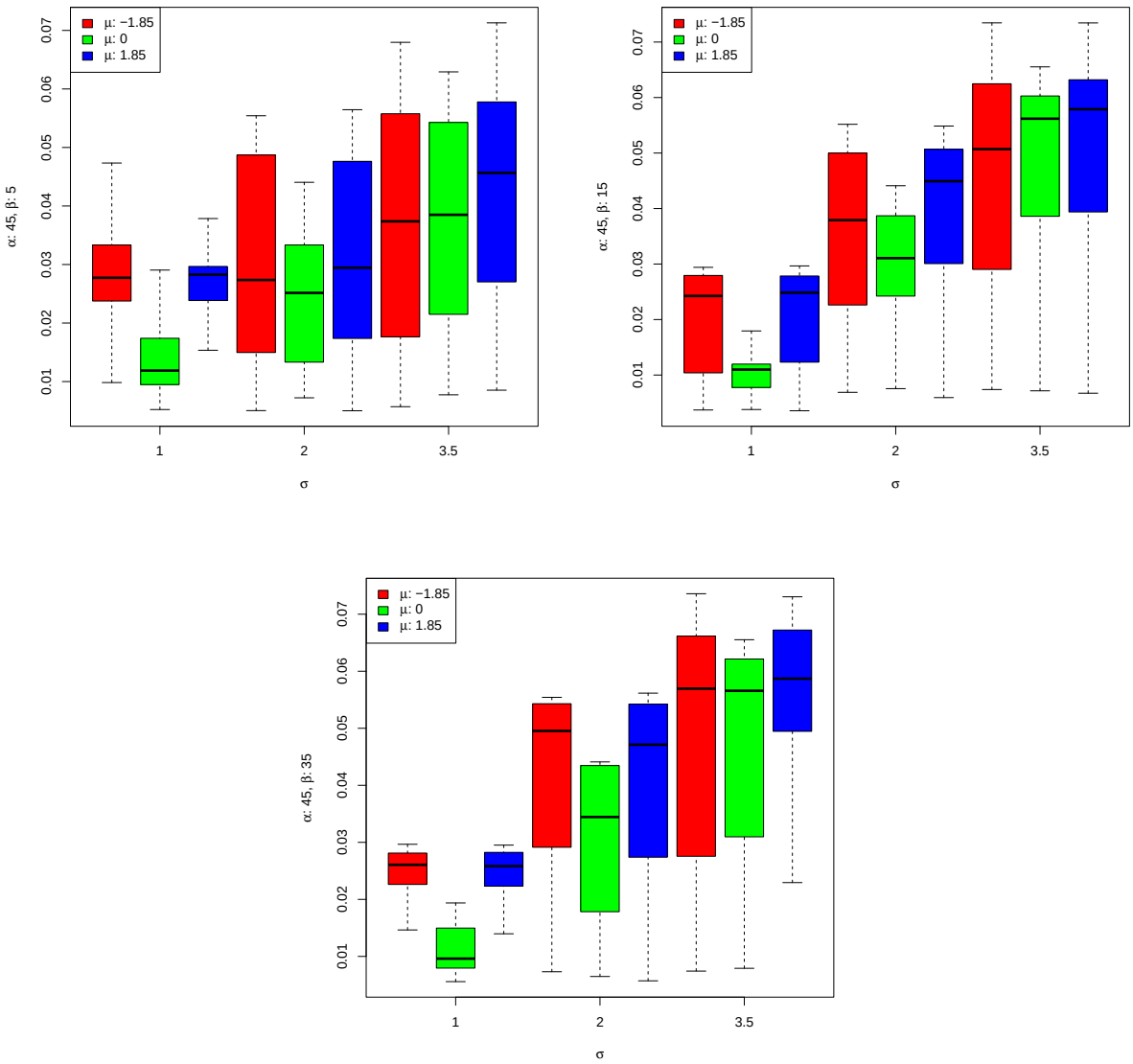

Figure S.18: Boxplots for the estimated total variation (TV) distance in the DA analysis for $\mathcal{LGN}(\mu, \sigma)$ (continuation).

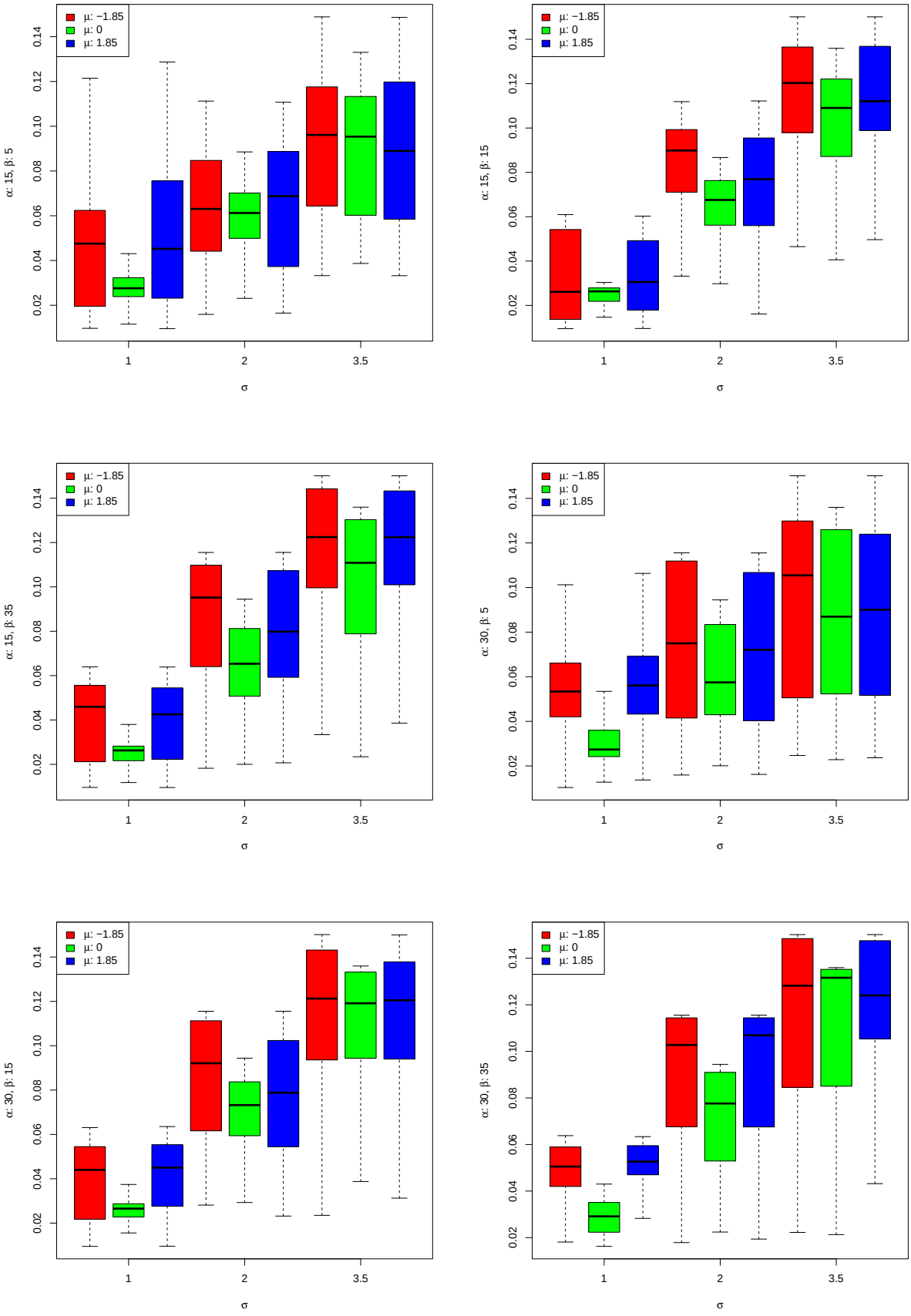

Figure S.19: Boxplots for the estimated Hellinger distance (HD) in the DA analysis for $\mathcal{LGN}(\mu, \sigma)$.

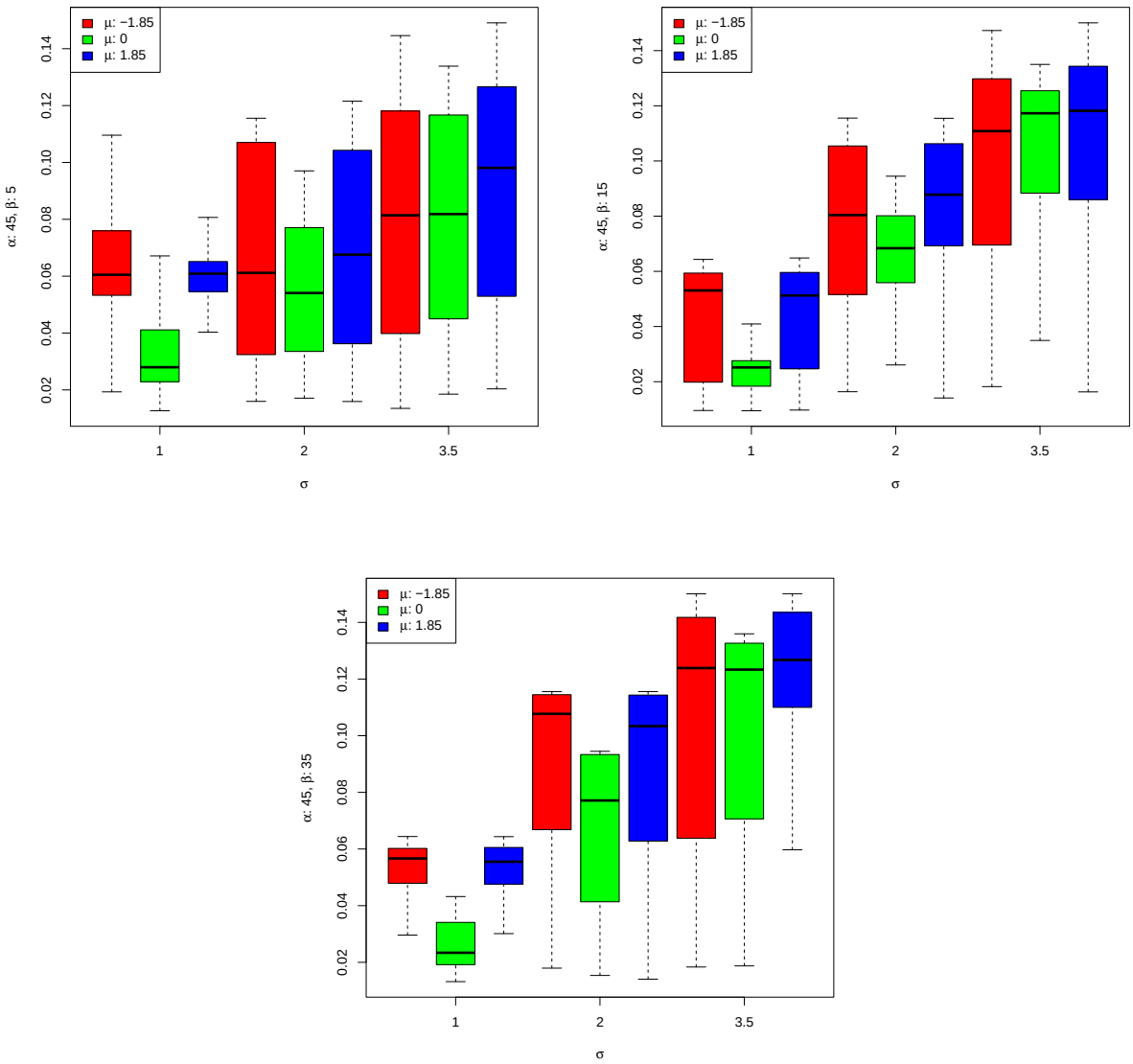

Figure S.20: Boxplots for the estimated Hellinger distance (HD) in the DA analysis for $\mathcal{LGN}(\mu, \sigma)$ (continuation).

2 Extended results for Section 6 (Applications)

This section contains extended numerical as well as graphical results for the case study described in Section 6.4.

2.1 Case study: posterior predictive check

Figure S.21 illustrates the results for the statistics being used for the PPC analysis. In this case, the posterior predictive analysis suggests a quite satisfactory goodness-of-fit, with the predicted fuzzy data closely matching the observed data across all evaluated metrics (centroids: CP = 0.95, bP = 0.02; supports: CP = 0.91, bP = 0.04 and fuzziness: CP = 0.92, bP = 0.04). These results indicate that the final model does not fail to capture the three characteristics of the observed data.

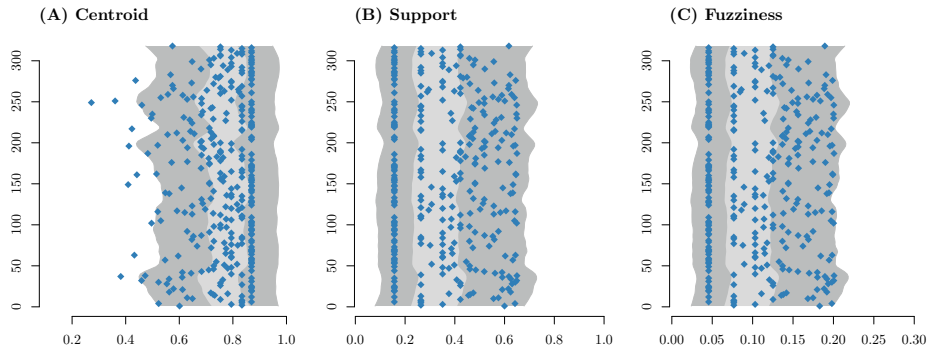

Figure S.21: Case study – Panels (A)-(C) illustrate the interquartile range (light gray area), the max-min range (dark gray area), and the defuzzified observed data (blue dots) for each of the posterior predictive statistics. The horizontal axis represents the scale of the response variable Y, while the vertical axis corresponds to the statistical units.

2.2 Case study: comparisons of fuzzy regression methods

The aim of this analysis is that of comparing the proposed conditional model (fCM) with some state-of-art regression methods. Since our model deals with fuzzy outcome variables $\tilde{\mathbf{y}}$ and non-fuzzy predictors $\mathbf{X}$, four methods were selected for an adequate comparison: the interactive fuzzy-output/crisp-input linear regression proposed by D'Urso [1] (fOLS); the classic Tanaka's possibilistic linear regression [2] (PLR); the multi-objective fuzzy linear regression developed by Nasrabadi et al. [3], which fits the mode of the observed fuzzy numbers via least squares while fitting the spread component by means of the possibilistic approach (MOFLR); the fuzzy rule-based system for regression tasks [4] (FRBS), which offers an alternative model-free method to learn the linear regression function given a learning set. The four methods were applied on the sexual intimacy dataset and the results were compared to those obtained by our conditional model. Since our proposal is based on a generative probabilistic model, which represents a novelty not present in previous approaches, an adequate comparison would require a method

to consistently generate new data from the fitted model for the competing methods as well. In addition, the standard approaches considered here also lack a consistent way to compute the variance of the fuzzy estimators. Therefore, while this latter would be approximated using bootstrap [5, 6], for lack of a probablistic generative model, the goodness-of-fit of the standard methods is evaluated by constrasting the fitted fuzzy numbers $\hat{\tilde{\mathbf{y}}}$ with the observed ones $\tilde{\mathbf{y}}$. The following measures were used:

- the Bertoluzza's distance between two fuzzy sets:

$$D_{\xi}^{\lambda}\ (\hat{\tilde{y}}, \tilde{y}) = \left(\int_0^1 \left(\text{mid}\ \hat{\tilde{y}}(\alpha) - \text{mid}\ \tilde{y}(\alpha) \right)^2 + \xi \left(\text{spr}\ \hat{\tilde{y}}(\alpha) - \text{spr}\ \tilde{y}(\alpha) \right)^2\ d\lambda(\alpha) \right)^{\frac{1}{2}}$$

  where mid $\tilde{z}$ denotes the midpoint of the α-cut $z(\alpha)$ of the fuzzy set $\tilde{z}$ (e.g., a real interval) whereas spr $\tilde{z}$ is its length, ξ is a positive weight (e.g., $\xi = \frac{1}{3}$), and λ is a weighting function for the α cut (usually, it is an identity function) [7];

- the ratio between the fuzziness of two fuzzy sets:

$$w(\hat{\tilde{y}}, \tilde{y}) = 1 - \frac{\int_0^1 \left(\hat{\tilde{y}}_u(\alpha) - \hat{\tilde{y}}_l(\alpha) \right)}{\int_0^1 \left(\tilde{y}_u(\alpha) - \tilde{y}_l(\alpha) \right)}$$

  where $z(\alpha)$ indicates the α-cut of the fuzzy set $\tilde{z}$, with l and u denoting its lower and upper bounds, respectively [8].

An additional measure used to evaluate the consistency of the results obtained by standard methods is to evaluate how many times the assumptions $s > 0$ and $m \in [lb, ub]$ for fuzzy data are being violated (in the case study, $lb = 1$ and $ub = 5$). Finally, in the model comparison, it should be noted that for the proposed fCM the fitted values $\widehat{\widetilde{\mathbf{Y}}}$ is a $n \times B$ matrix containing B random instances of n fuzzy numbers, which is obtained by running the estimated model B times as for the PPC analysis.

Tables S.21 shows the estimated regression coefficients alongside their standard errors and 95% confidence intervals for all the regression methods being considered. In the case of fCM, the estimated regression coefficients and their standard errors are computed using the marginal posterior distributions while the reported confidence intervals represent highest density intervals (HDIs). For the FRBS regression, estimated coefficients are not reported as this method models the linear function using a fuzzy inference system. Unlike for the fCM case, which adopts a probabilistic framework to model modes and spreads of the observed fuzzy data, the alternative regression methods explicitly provide regression equations for the left and right spread components (PLR and MOFLR model symmetric fuzzy numbers and require a regression coefficient for the total spread only). As expected, the results in terms of estimated models largely differ, as they are based on a quite different rationale. Figures S.22-S.25 and table S.2 report the results of the Bertoluzza's distance and fuzziness ratio between the observed and fitted fuzzy data for all the regression methods under consideration. Overall, the proposed fCM regression

outperforms the alternative regression methods both in terms of goodness-of-fit (measured via the Bertoluzza's distance) and fuzziness reconstruction. Particularly, PLR and MOFLR severely understimate the observed fuzziness. On the contrary, FRBS overestimates fuzziness. Only the fOLS regression provides a biased but still consistent fuzziness reconstruction, close to what fCM does. However, this regression method produces incosistent fitted values, with 129 out of $n = 318$ violations (see Table S.3).

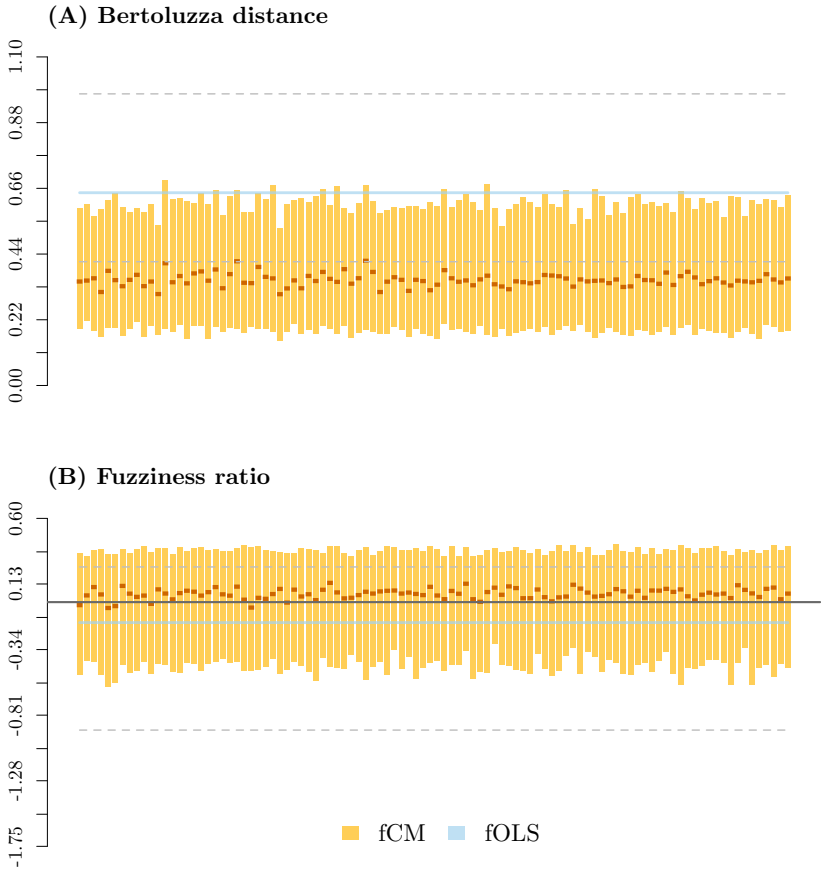

Figure S.22: Case study (fCM vs. fOLS) – Panels (A)–(B) illustrate the Bertoluzza distance and the fuzziness ratio for the proposed fCM method ($B = 100$ colored boxplots) and the fOLS regression approach (1st, 2nd, and 3rd quantiles represented as horizontal colored lines). The horizontal axis corresponds to the $B = 100$ replicates for fCM, while the vertical axis represents the scale of the comparison metric. Note that in Panel (B), the solid dark horizontal line is drawn at $y = 0$, which marks the case where the fuzziness of fitted and observed fuzzy data is equal.

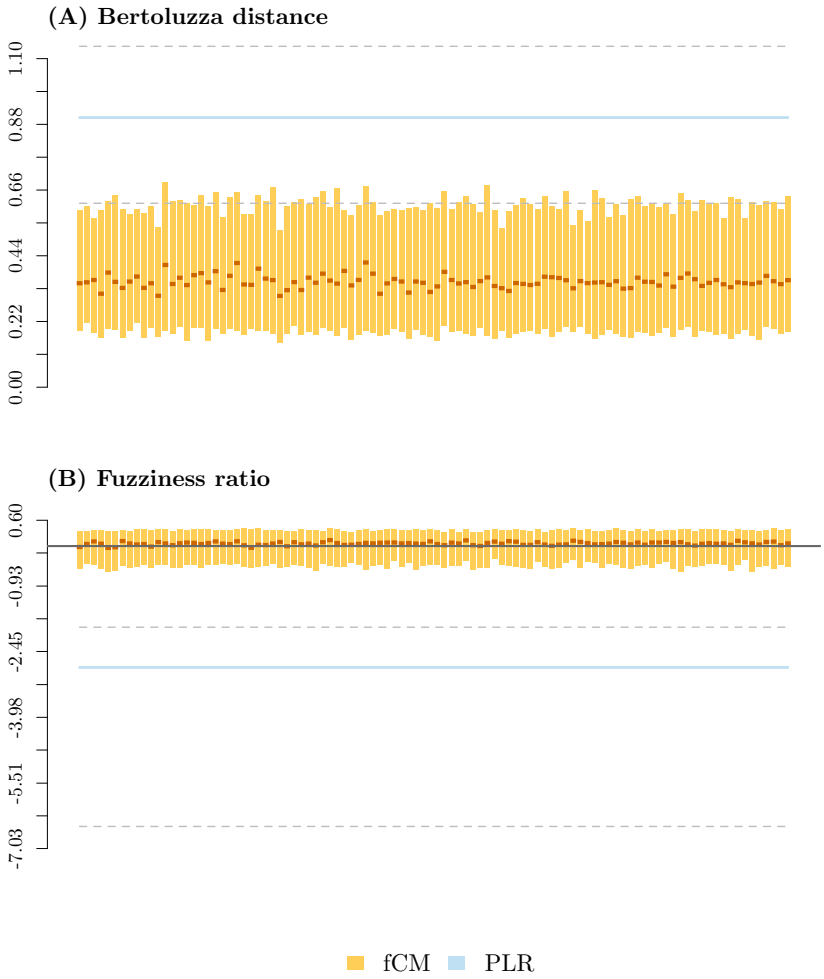

Figure S.23: Case study (fCM vs. PLR) – Panels (A)–(B) illustrate the Bertoluzza distance and the fuzziness ratio for the proposed fCM method ($B = 100$ colored boxplots) and the PLR approach (1st, 2nd, and 3rd quantiles represented as horizontal colored lines). The horizontal axis corresponds to the $B = 100$ replicates for fCM, while the vertical axis represents the scale of the comparison metric. Note that in Panel (B), the solid dark horizontal line is drawn at $y = 0$, which marks the case where the fuzziness of fitted and observed fuzzy data is equal.

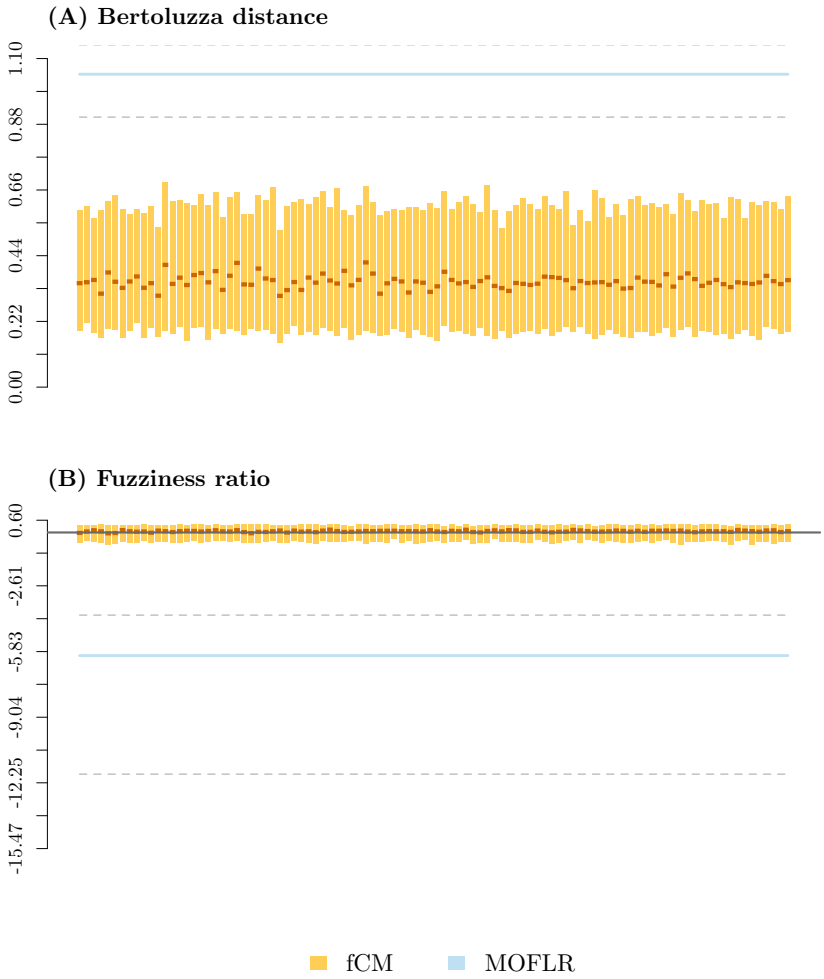

Figure S.24: Case study (fCM vs. MOFLR) – Panels (A)–(B) illustrate the Bertoluzza distance and the fuzziness ratio for the proposed fCM method ($B = 100$ colored boxplots) and the MOFLR approach (1st, 2nd, and 3rd quantiles represented as horizontal colored lines). The horizontal axis corresponds to the $B = 100$ replicates for fCM, while the vertical axis represents the scale of the comparison metric. Note that in Panel (B), the solid dark horizontal line is drawn at $y = 0$, which marks the case where the fuzziness of fitted and observed fuzzy data is equal.

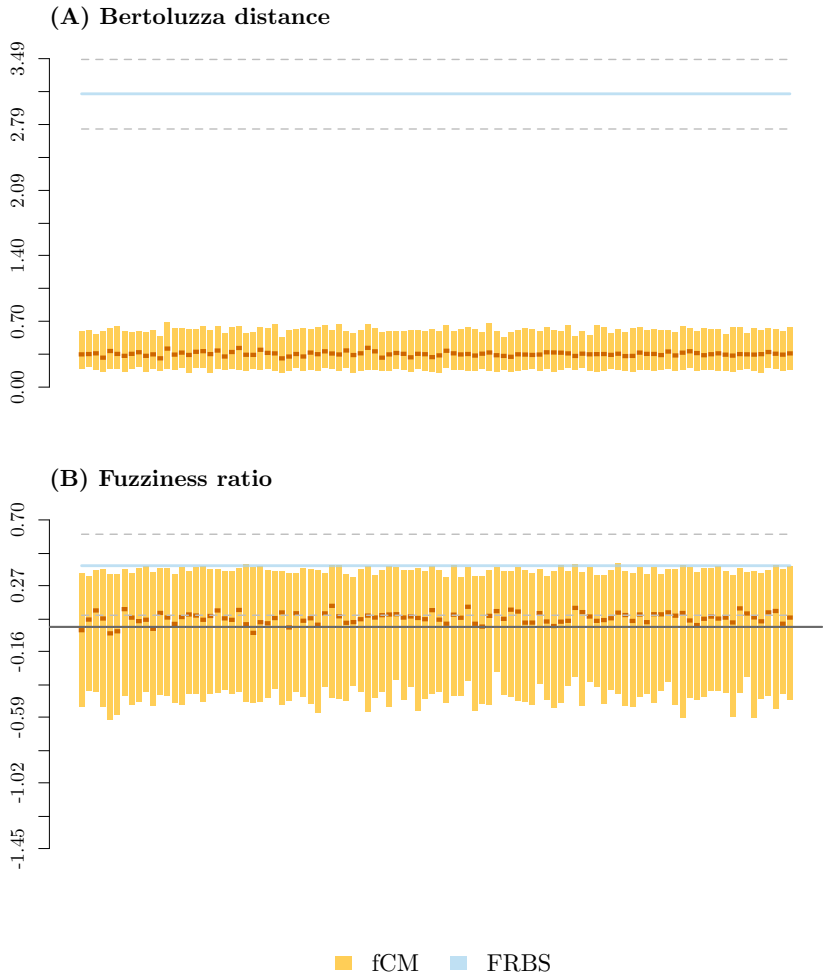

Figure S.25: Case study (fCM vs. FRBS) – Panels (A)–(B) illustrate the Bertoluzza distance and the fuzziness ratio for the proposed fCM method ($B = 100$ colored boxplots) and the FRBS regression approach (1st, 2nd, and 3rd quantiles represented as horizontal colored lines). The horizontal axis corresponds to the $B = 100$ replicates for fCM, while the vertical axis represents the scale of the comparison metric. Note that in Panel (B), the solid dark horizontal line is drawn at $y = 0$, which marks the case where the fuzziness of fitted and observed fuzzy data is equal.

		$\hat{\beta}$	$\hat{\sigma}_\beta$	95% CI lb	95% CI ub
fCM	β_0	1.15	0.03	1.09	1.22
	$\beta_{\texttt{age}}$	0.04	0.04	-0.04	0.13
	$\beta_{\texttt{rel\_length}}$	-0.03	0.04	-0.11	0.07
	$\beta_{\texttt{sex\_desire}}$	0.04	0.03	-0.03	0.10
	$\beta_{\texttt{gender\_partner:female}}$	0.40	0.03	0.33	0.46
	$\beta_{\texttt{respo\_partner}}$	-0.01	0.03	-0.07	0.06
fOLS	β_0	4.63	0.36	3.98	5.47
	$\beta_{\texttt{age}}$	0.32	0.19	-0.46	0.36
	$\beta_{\texttt{rel\_length}}$	1.06	0.18	-0.25	0.49
	$\beta_{\texttt{desire}}$	0.43	0.12	-0.28	0.22
	$\beta_{\texttt{gender\_partner:female}}$	0.47	0.13	-0.14	0.42
	$\beta_{\texttt{partner\_respo}}$	0.74	0.14	-0.11	0.42
	β_l	0.11	0.03	0.14	0.26
	β_r	0.05	0.16	1.49	2.14
PLR (mode)	β_0	3.33	0.12	2.97	3.25
	$\beta_{\texttt{age}}$	0.06	0.04	-0.06	0.14
	$\beta_{\texttt{rel\_length}}$	-0.05	0.05	-0.09	0.12
	$\beta_{\texttt{desire}}$	0.02	0.04	-0.10	0.08
	$\beta_{\texttt{gender\_partner:female}}$	-0.02	0.06	-0.08	0.17
	$\beta_{\texttt{partner\_respo}}$	0.12	0.05	-0.15	0.08
PLR (spread)	β_0	1.80	0.12	1.82	2.17
	$\beta_{\texttt{age}}$	0.00	0.04	0.00	0.14
	$\beta_{\texttt{rel\_length}}$	0.00	0.04	0.00	0.13
	$\beta_{\texttt{desire}}$	0.04	0.04	0.00	0.12
	$\beta_{\texttt{gender\_partner:female}}$	0.00	0.06	0.00	0.20
	$\beta_{\texttt{partner\_respo}}$	0.10	0.04	0.00	0.16
MOFLR (mode)	β_0	4.04	0.03	3.98	4.09
	$\beta_{\texttt{age}}$	0.03	0.04	-0.07	0.06
	$\beta_{\texttt{rel\_length}}$	-0.02	0.04	-0.07	0.07
	$\beta_{\texttt{desire}}$	0.04	0.03	-0.06	0.06
	$\beta_{\texttt{gender\_partner:female}}$	-0.01	0.03	-0.06	0.06
	$\beta_{\texttt{partner\_respo}}$	0.34	0.03	-0.06	0.06
MOFLR (spread)	β_0	3.29	0.24	3.26	4.17
	$\beta_{\texttt{age}}$	-0.33	0.15	-0.28	0.29
	$\beta_{\texttt{rel\_length}}$	0.23	0.14	-0.28	0.25
	$\beta_{\texttt{desire}}$	0.33	0.15	-0.30	0.30
	$\beta_{\texttt{gender\_partner:female}}$	-0.05	0.19	-0.38	0.39
	$\beta_{\texttt{partner\_respo}}$	0.38	0.13	-0.27	0.24

Table S.1: Case study — Estimated regression coefficients $\hat{\beta}$, standard errors $\hat{\sigma}_\beta$, and 95% confidence intervals for the proposed fCM regression and the competing regression methods. In the fCM case, the estimated coefficients and standard errors correspond to posterior quantities, and the reported confidence intervals represent highest density intervals (HDIs). Estimated coefficients are not reported for the FRBS regression method, as it models the linear function via a fuzzy inference system rather than explicit parameter estimation.

		Min.	1st Qu.	Median	Mean	3rd Qu.	Max.
Bertoluzza's distance	fCM	0.26	0.35	0.40	0.44	0.47	1.25
	fOLS	0.04	0.41	0.65	0.75	0.98	2.91
	PLR	0.24	0.62	0.90	0.87	1.14	1.37
	MOFLR	0.36	0.90	1.05	1.01	1.15	1.57
	FRBS	0.59	2.74	3.12	2.96	3.48	3.58
Fuzziness ratio	fCM	-1.23	-0.82	0.05	-0.18	0.23	0.44
	fOLS	-5.18	-0.92	-0.15	-0.37	0.25	1.00
	PLR	-7.14	-6.52	-2.82	-3.64	-1.89	-0.90
	MOFLR	-17.16	-11.83	-6.02	-7.61	-4.04	-0.50
	FRBS	-10.38	0.08	0.40	-0.46	0.61	0.70

Table S.2: Case study – Summary statistics of the performance of the regression methods measured in terms of Bertoluzza's distance and fuzziness ratio between observed and fitted fuzzy data.

	$y_c < lb$	$y_c > ub$	$y_l < 0$	$y_r < 0$
fOLS	6	121	1	1
PLR	0	0	0	0
MFLR	0	0	0	0
FRBS	305	0	0	0

Table S.3: Case study – Constraints violation frequency for the alternative regression methods. Note that in this case $lb = 1$ and $ub = 5$, whereas $n = 318$.

3 Assessing model mispecifications

The probabilistic schema proposed to represent the epistemic fuzzification procedure is based on the general idea that each fuzzy observation $\tilde{y}_i = (m_i, s_i)$ is interpreted as an imprecise measurement of an unobserved realization Y_i, blurred by the epistemic uncertainty S_i. This mechanism is formalized as a hierarchical two-stage model, where the support of the observed fuzzy number $\tilde{y}_i$ includes the true unobserved realization y_i with high possibility. This implies that $\mathbb{E}[M_i] = \mathbb{E}[Y_i]$ and $\mathbb{V}\mathrm{ar}[M_i] = g(\mathbb{E}[Y_i], \mathbb{V}\mathrm{ar}[Y_i], c)$, with c being a scaling factor (for further results, see Section 3.2 of the article). Thus, the proposed hierarchical model imposes a constraint on the support of fuzzy realizations, namely $\mathrm{Sup}(Y) \subseteq \mathrm{Sup}(M)$, which is guaranteed as long as $S \perp\!\!\!\perp Y$.

However, the proposed model does not account for situations where $\mathrm{Sup}(Y) \nsubseteq \mathrm{Sup}(M)$, which would imply a fuzzification mechanism with more than two stages. This scenario also includes cases in which the observed fuzzy datum $\tilde{y}_i$ does not contain the true unobserved realization y_i even with low possibility. Although not frequent, such cases may occur in human rating contexts, where judgments are systematically affected by cognitive biases, affective framing, anchoring effects, or contextual cues [9]. These distortions may cause the reported fuzzy number to systematically misrepresent the true internal judgment — for example, by shifting the mode and support upward due to branding effects or overconfidence [10]. Note that this second-stage blurring may act on the mode m, on the spread s, or on both components simultaneously. In what follows we consider the first case only, where the second-stage blurring acts on m and it is independent from Y and S. Although simple, this condition is typical of situations involving two distinct error processes: one acting by increasing the fuzziness of the fuzzy datum, and the other by distorting its mode. For the sake of simplicity, consider $\mathrm{Sup}(Y) = \mathbb{R}$ and $\delta \in \mathbb{R}$. Then, under the usual assumptions of independence among the hierarchical components, $Y \perp\!\!\!\perp S$, the conditional equation of the observed mode is given by

$$m_i | s_i, y_i, \delta_i \sim \mathcal{B}_{4P}\left(m; s_i(y_i + \delta_i), s_i - s_i(y_i + \delta_i), lb, ub\right), \tag{S.1}$$

which accommodates the idea of systematic distortions affecting the true unobserved realization before fuzzification. Consequently,

$$\begin{aligned}
&\mathbb{E}[M_i] = \mathbb{E}[Y_i] + \delta_i, \\
&\mathbb{V}\mathrm{ar}[M_i] = (\mathbb{V}\mathrm{ar}[Y_i] - \mathbb{V}\mathrm{ar}[Y_i]\, c) + \mathbb{E}[Y_i](1 - \mathbb{E}[Y_i])c + \delta_i(1 - \delta_i)c,
\end{aligned}$$

where c is defined as in the Appendix of the article. Although δ_i can be defined as a random quantity, the simplest case where δ_i is a constant, is sufficient to represent the desired scenario in which the observed fuzzy datum does not contain the true unobserved realization, i.e., $y_i \notin \tilde{A}_0^{(i)}$. As one might expect, applying our original method to estimate the parameters of a δ-shifted sample of fuzzy data would produce biased results. To illustrate this, consider the following case

study with synthetic data.[1]

The matrix $\mathbf{X}_{n\times J}$, with $n = 250$ and $J = 3$, contained two continuous predictors (generated uniformly into the interval $(-1, 1)$ and then standardized) and a categorical predictor with two levels ($n_A = 132$ and $n_B = 118$). The true unobserved model was set to be Gaussian $f_Y(\mathbf{y}; \boldsymbol{\mu}^0, \mathbf{I}\phi^0)$, with $\boldsymbol{\mu}^0 = \mathbf{X}\boldsymbol{\beta}^0$ (the numeric assignment for $\boldsymbol{\beta}^0$ and ϕ^0 are reported in the first column of Table S.4). The unobserved realizations $\mathbf{y}^0_{250\times 1}$ showed the following quantiles: -20.222 (min), -4.737 ($q_{0.25}$), 0.885 ($q_{0.50}$), 0.867 (mean), 5.763 ($q_{0.75}$), 21.137 (max). The systematic shift from $\mathbb{E}[Y]$ was $\delta = 11.673$ and the shifted random vector was generated using a truncated Gaussian model $\mathbf{y} \sim \mathcal{N}(y; \mathbf{y}^0 + \delta, \mathbf{I}\sigma^0)_{[\min(\mathbf{y}^0),\max(\mathbf{y}^0)]}$, with $\sigma^0 = 1.5$. Finally, the vector of observed spreads was generated using a Gamma distribution $s \sim \mathcal{G}(s; \alpha_s, \beta_s)$, with $\alpha_s = 25.0$ and $\beta_s = 0.5$ whereas the observed modes were generated using Eq. (S.1). The quantiles of the observed modes $\mathbf{m}_{250\times 1}$ were as follows: -9.029 (min), 7.180 ($q_{0.25}$), 12.216 ($q_{0.50}$), 11.922 (mean), 18.010 ($q_{0.75}$), 21.198 (max). The number of observed fuzzy data not containing the true unobserved signal y^0 is equal to 102 (40.8%).

The approximated Gibbs sampler described in Section 4 of the main article was run with ten independent chains of 2000 samples each (burn-in period: 1000 samples). Weakly informative priors were used, and the lower and upper bounds of the observed modes were computed as specified in Section 3.3.4 of the main article. As $f_Y(y; \boldsymbol{\theta}_y)$ is a real unbounded model, the linear predictor $\eta_i = g(\boldsymbol{\mu}_i)$ was modeled using the identity function. All the chains reached convergence according to Gelman and Rubin's $\widehat{R}$ index and were subsequently used in the data analysis. Table S.4 reports some of the posterior statistics, along with the 95% Highest Posterior Density Interval (HPDI) bounds. As largely expected, most of the posterior quantiles are biased, and the marginal posterior distributions also show a higher level of variance. Figure S.26 shows the results of a PPC analysis for the misspecified model ($B = 500$). The analysis reveals a poor fit of the model in reconstructing two of the key observed quantities: fuzziness and support. Indeed, although the posterior analysis for the centroids is not dramatically affected by the misspecification (CP=0.94, bP=0.04), this largely affected the supports (CP=0.43, bP=0.24) and the fuzziness (CP=0.64, bP=0.15). The same applies to the model-implied predictions $\hat{\mathbf{y}}_{250\times 1}$ (see Figure S.27). In this case, the predictions provided by the estimated model grossly diverge from the true realizations $\mathbf{y}^0$, especially with regard to the mean and the variance of $f_Y(y; \boldsymbol{\theta}_y)$.

	true	mean	sd	HDI lb	HDI ub
β_0	2.38	11.54	0.53	10.46	12.55
β_1	-3.10	-2.61	0.64	-3.88	-1.38
β_3	-2.68	-2.02	0.68	-3.34	-0.70
β_4	-3.26	-0.81	0.75	-2.28	0.66
ϕ	1.87	1.85	0.04	1.79	1.93

Table S.4: Posterior quantiles and 95% HPDIs for the model parameters. Note that the true parameters are reported in the second column, colored in gray.

[1]The detailed script used for this study is available at the repository indicated in the main article.

On the whole, model misspecifications can be assessed by means of posterior predictive analyses, as shown in this short case study. When the observed fuzzy data do not align with the two-stage blurring mechanism assumed by the proposed model – as is the case for δ-shifted fuzzy observations – inspecting the marginal posterior densities of the model parameters (e.g., their variance), as well as running posterior predictive checks, can help in evaluating whether model assumptions generally hold for the sample of data under consideration.

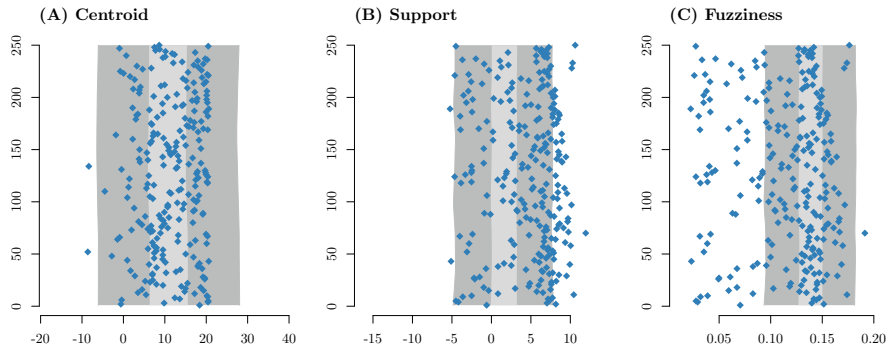

Figure S.26: PPC analysis – Panels (A)-(C) illustrate the interquartile range (light gray area), the max-min range (dark gray area), and the defuzzified observed data (blue dots) for each of the posterior predictive statistics. The horizontal axis represents the scale of the response variable Y, while the vertical axis corresponds to the statistical units.

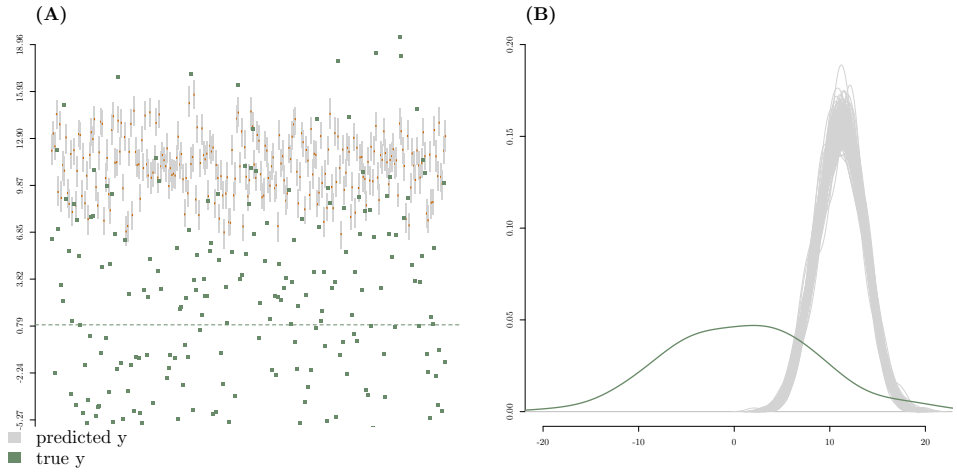

Figure S.27: PPC analysis – Panel (A) reports the true unobserved and not shifted realizations $\mathbf{y}^0$ (green squares) against the model-implied predictions $\hat{\mathbf{y}}$ (gray boxplots); the dotted horizontal line is drawn at $\mathbb{E}\left[Y^0\right]$. Panel (B) reports the same information but now in terms of densities. Note that, in both cases, $B = 500$ predictions of size n were realized.

References

[1] P. D'Urso, Linear regression analysis for fuzzy/crisp input and fuzzy/crisp output data, Computational Statistics & Data Analysis 42 (1-2) (2003) 47–72.

[2] H. Tanaka, I. Hayashi, J. Watada, Possibilistic linear regression analysis for fuzzy data, European Journal of Operational Research 40 (3) (1989) 389–396.

[3] M. M. Nasrabadi, E. Nasrabadi, A. R. Nasrabady, Fuzzy linear regression analysis: a multi-objective programming approach, Applied mathematics and computation 163 (1) (2005) 245–251.

[4] L. S. Riza, C. Bergmeir, F. Herrera, J. M. Benítez, frbs: Fuzzy rule-based systems for classification and regression in r, Journal of statistical software 65 (2015) 1–30.

[5] P. Grzegorzewski, M. Romaniuk, Bootstrap methods for epistemic fuzzy data, International Journal of Applied Mathematics and Computer Science 32 (2) (2022) 285–297.

[6] M. Romaniuk, P. Grzegorzewski, Resampling fuzzy numbers with statistical applications: `FuzzyResampling` package., R J. 15 (1) (2023) 271–283.

[7] M. R. Casals Varela, N. O. Corral Blanco, M. Á. Gil Álvarez, M. T. López García, M. A. Lubiano Gómez, M. F. Montenegro Hermida, M. G. Naval Alegre, A. J. Salas Riesgo, et al., Bertoluzza et al.'s metric as a basis for analyzing fuzzy data, METRON: International Journal of Statistics, 71 (3) (2013).

[8] P. Grzegorzewski, O. Hryniewicz, M. Romaniuk, Flexible resampling for fuzzy data, International Journal of Applied Mathematics and Computer Science 30 (2) (2020) 281–297.

[9] K. Zupanc, E. Štrumbelj, A bayesian hierarchical latent trait model for estimating rater bias and reliability in large-scale performance assessment, Plos one 13 (4) (2018) e0195297.

[10] J. Mikhaeil, A. Gelman, P. Greengard, Hierarchical bayesian models to mitigate systematic disparities in prediction with proxy outcomes (2024). `arXiv:2403.00639`.
URL `https://arxiv.org/abs/2403.00639`